IJEMME

INTERNATIONAL JOURNAL of ELECTRONICS, MECHANICAL and MECHATRONICS ENGINEERING

Year: **2020** Volume **10** Number **1**

VISUAL DESIGN & ACADEMIC STUDIES COORDINATION OFFICE

Nabi SARIBAŞ - Selin YILMAZ - Elif ERMAN

PRINTED BY

Renk Matbaası Basım ve Ambalaj San. Tic. A.Ş.
Ziya Gökalp Mah. Süleyman Demirel Bulvarı İş Modern D Blok No:27D D:D8 34104 Başakşehir / İstanbul

ISSN: 2146-0604

International Journal of Electronics, Mechanical and Mechatronics Engineering (IJEMME) is peer-reviewed journal which provides a platform for publication of original scientific research and applied practice studies. Positioned as a vehicle for academics and practitioners to share field research, the journal aims to appeal to both researchers and academicians.

Internationally indexed by EBSCO and DOAJ

CONTENTS

From the Editor

International Journal of Electronics, Mechanical and Mechatronics Engineering (IJEMME), is an international multi-disciplinary journal dedicated to disseminate original, high-quality analytical and experimental research articles on Robotics, Mechanics, Electronics, Telecommunications, Control Systems, System Engineering, Biomedical and Renewable Energy Technologies. Contributions are expected to have relevance to an industry, an industrial process, or a device. Subject areas could be as narrow as a specific phenomenon or a device or as broad as a system.

The manuscripts to be published are selected after a peer review process carried out by our board of experts and scientists. Our aim is to establish a publication which will be abstracted and indexed in the Engineering Index (EI) and Science Citation Index (SCI) in the near future. The journal has a short processing period to encourage young scientists.

Prof. Dr. Hasan HEPERKAN
Editor

INTERNATIONAL JOURNAL OF ELECTRONICS, MECHANICAL AND MECHATRONICS ENGINEERING
Vol.10 Num.1 - 2020 (1763 - 1784)

Received: 15.11.2019
Accepted: 20.12.2019

The Effect of Different Mppt on the Linear Load and Non-Linear Load in Pv System

Halmat SAEED[1], Murtaza FARSADI[2]

Abstract - The output power of a PV array is dependent on environmental factors such as solar irradiation and temperature. So, it has a non-linear I-V characteristic. Maximum Power Point (MPP) is a point on the I-V, P-V characteristic curve of a PV array where the PV device generates maximum output power. The location of MPP shifts as the climate changes. MPPT's aim is to keep the solar operating voltage as similar to MPP as possible under changing environmental conditions. They must run at their MPPT considering the inhomogeneous shift in environmental conditions in order to continuously gather the full power from the PV array. Here the most commonly used MPPT algorithms for PV applications are illustrated because they are easy to implement which are Perturb and Observe (P&O), Hill Climbing (HC) and Incremental Conductance (INC). In this paper, the applications of those three MPPT algorithms in PV systems at linear and nonlinear loads have been investigated. Comparative analysis has been done and the efficient one based on different testing scenarios has been determined based on output results.

Key Words: *MPPT, PV System, linear load, non-linear load*

1. Introduction:

Nowadays the hot topic in the world is climate change. One of the main causes of climate change is using fossil fuels. One of the most widely used effective ways to tackle climate change issues is the installation of renewable energy sources including PV systems. [1]It is clean, free, and renewable. There are two types of photovoltaic systems: standalone and grid-connected PV

[1] *Istanbul Aydin University Department of Electrical and Electronics Engineering, Istanbul Turkey, halmatsaeed@stu.aydin.edu.tr, ORCID: 0000-0003-0379-8305*
[2] *Istanbul Aydin University Department of Electrical and Electronics Engineering, Istanbul Turkey, murtazafarsadi@aydin.edu.tr, ORCID: 0000-0001-7408-6597*
DOI: 10.17932/IAU.IJEMME.2010.001/ijemme_v10i1001

systems. Stand-alone photovoltaic systems are used for locations that are not connected to the electrical grid. The performance of the PV system in these systems is determined by the operating conditions. The maximum power point (MPP) PV source can be affected by three factors: radiation, load characteristics, and temperature. A grid-connected PV system is used in locations with easy access to the connected electrical network.

To generate the maximum power by the solar module, it is essential to find the point on the I-V characteristic where the current and voltage are at their maximum value continuously. This point is called the maximum power point (MPP). PV model is able to extract maximum available power if it is working on MPP point. Therefore, it is essential to use a maximum power point tracker (MPPT) with PV system to ensure the operation of the PV module at MPP. The two main dependent parameters in solar power are irradiance and temperature, which are not remaining stable due to continuous changes in the weather condition. At satisfying weather conditions, when the temperature and irradiance are good the PV model can generate maximum power efficiently while an effective MPPT algorithm is used with the system. There are many MPPT algorithms developed by researchers all over the world such as Differential method, Incremental Conductance (INC), Perturb and Observe (P & O) Fuzzy logic, Hill Climbing (HC). In this paper the focus will be on the application of P&O, (HC), and (INC). In PV system. The main contributions of this paper are:

- The application of the three mention MPPT at linear and non-linear load.
- Comparative analysis between them in terms of input and output Current, Voltage, and Power.
- The effect of changes in Irradiance and Temperature in the application of the proposed MPPTs at both sinarios (PV connected to linear load and PV connected to non-linear load.

The efficiency of solar power generation can be directly affected by the following factors:

- ✓ Irradiance and temperature
- ✓ PV panel cell.
- ✓ DC-DC converter
- ✓ Maximum Power Point Tracking (MPPT) algorithm.

2. Equivalent Circuit of a Solar Cell

The solar cell is a diode, and the diode is a p-n junction semiconductor. When the solar cell is exposed to the sunlight, a dc current is generated. The amount of current generated is proportionally varies with the solar irradiance. The performance of the pv module we can describe by a single standard diode model. Shown in figure(1) [2].

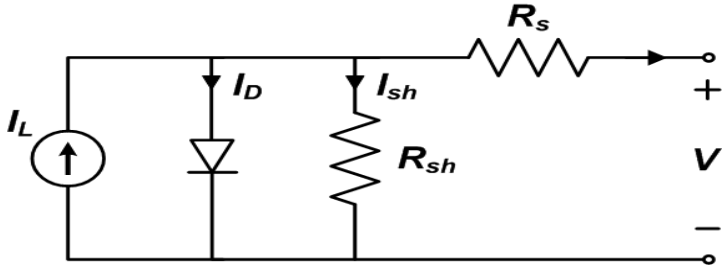

Figure 1: Equivalent circuit of a solar cell

The output current of the solar cell is can be represented by the following equation:

$$I = I_L - I_0 \left(e^{\frac{q(V-IR_S)}{AKT}} \right) - \frac{V-IR_s}{R_{sh}} \quad (1)$$

Where:

V = the output of the solar cell voltage.

I = the current output by the solar cell.

I_0 = a dark current saturation.

q = the number of electronic charge constant (1,602.10-19 Coulomb).

A = the ideality diode factor.

k = Boltzmain constant (1,38. 10-23 J/K).

Rsh = shunt resistance.

Rs = is the series resistance of the solar cell.

T = temperature of the cell [Kelvin].

The working of the shunt resistance (Rsh) is hard to explain. This is due to the imperfect nature of the p - n junction and the presence of inclusions near the edges of the cell providing a short junction path around the junction [1]. RS will be zero and RSH would be infinite in the ideal cell. But this is not possible in practice but in product we will try to minimize the effect of both resistances.

To simplify the solar cell in calculation (model) in we assume that the RSH is infinite, and we can neglect the effect of this resistor. Equation (1) could be simplified.

$$\boldsymbol{I \approx n_p I_L - n_p I_0 \left(e^{\frac{q(V-IR_S)}{AKTn_S}} - 1 \right)} \qquad (2)$$

Where:

np → number of solar cells in parallel

ns → number of solar cells in series

In any photovoltaic panel, many solar cells have been used, they are connected in a series and parallel as needed. In the end, the output voltage and current are large enough to connect with the grid or used by the equipment. By considering the simplification talked about above, we can show the characteristic of output voltage and current by equation (2) [8].

3. Irradiance & Temperature Effects

In the solar module, two factor irradiation and temperature directly effecting on the working of the panel. These two main reasons directly affecting on the working of the solar panel which is irradiation and temperature. As a result of any change in the irradiance and temperature affecting the output power of the panel, the MPPT is working to find the maximum available power in the panel and any change of radiation and temperature.

As was previously mentioned, the photo-generated current is directly proportional to the irradiance level, so an increment in the irradiation leads to a higher photo-generated current. Moreover, the short circuit current is directly proportional to the photo-generated current; therefore, it is directly proportional to the irradiance.

In normal operation of PV cell, the power generated an affected by irradiance of the cell as it is illustrated in eq (1), eq (2).

From the figure (2) it can be noticed the effect of changing temperature on the open voltage is very large but effect on current can be neglected theoretically. But, changing in irradiance on the PV panel on the short circuit (current) characteristic curve is logarithmic as shown in figure (4), eq (3) shows this relation the characteristic, carve bellow shows that in any change in irradiance directly affecting on the current generation by the panel. Any increase in current generation means an increase in power generated by the panel proportionally.

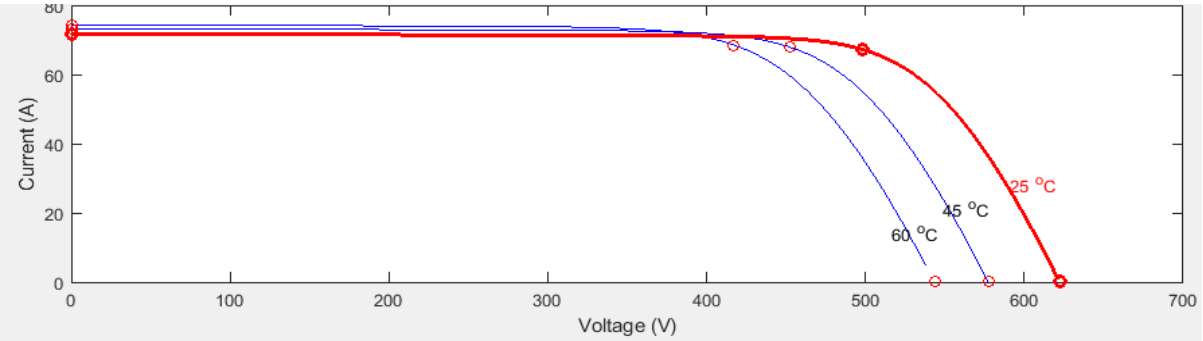

Figure 2. MPP changes with Temperature (I-V Curves)

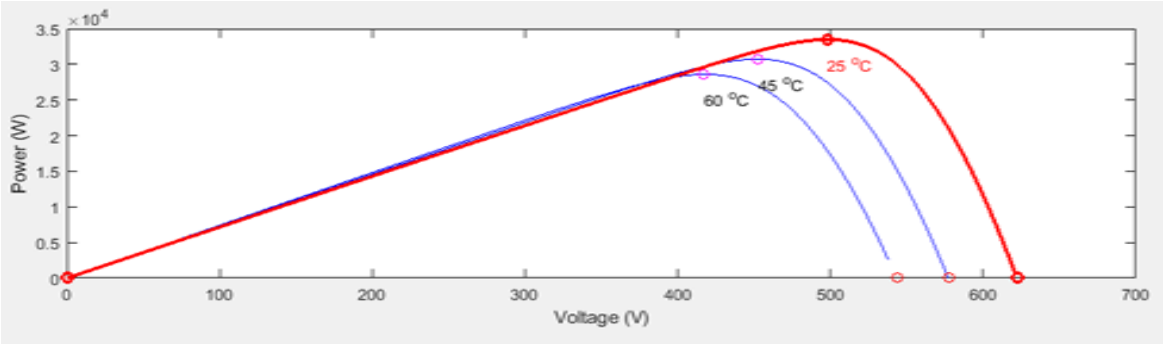

Figure 3. MPP changes with Temperature (P-V Curves)

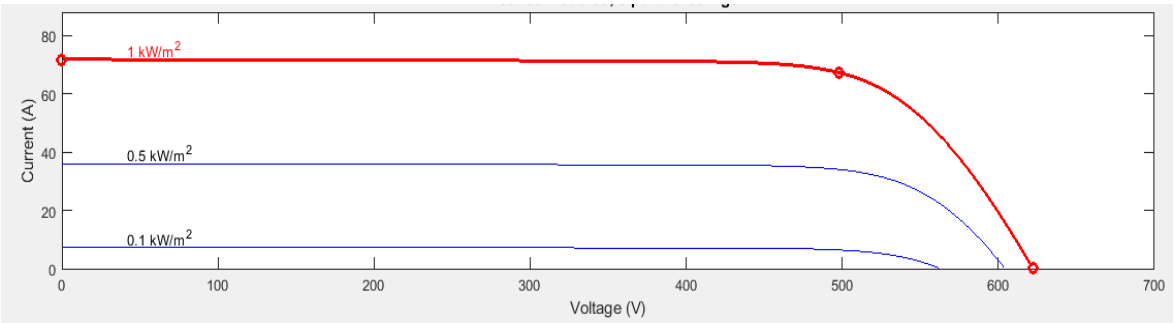

Figure 4. MPP changes with Irradiance levels (I-V Curves)

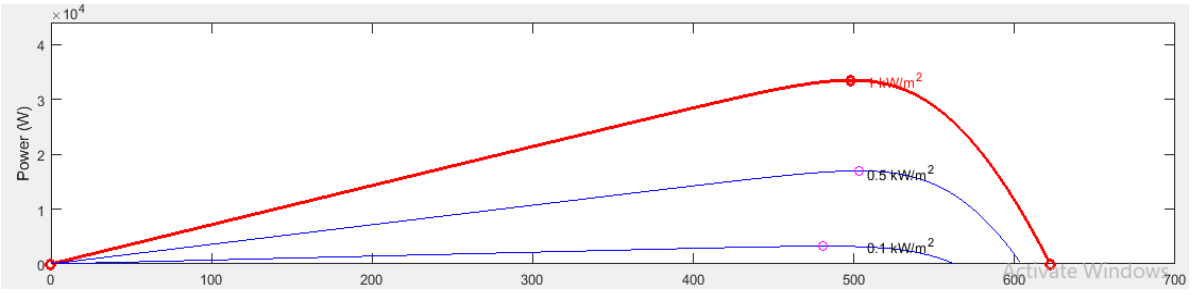

Figure 5. MPP changes with Irradiance levels (P-V Curves)

The effect of irradiance on the current is very bigger than the effect on the voltage as shown in figure (2,3,4,5), for that reason, the change in voltage by irradiance is neglected [6], when the irradiance is increasing the power generated is increase because voltage and current generated in this change are positive.

On the other hand, the voltage change is directly proportional with the temperature if the temperature is increasing the voltage generated is decrease, this equation is illustrating the effect of temperature on the $V_{OC.}$

$$\boldsymbol{V_{OC}(T) \approx V_{OC}^{STC} + \frac{K_{V\%}}{100}(T - 273.15)} \qquad \textbf{(3)}$$

As stated earlier, the effect temperature on both voltage and current is a different increase in temperature means a decrease in voltage much more than increasing in current so the power generated when the temperature is increase is smaller, figure (8) shows the effect of temperature on the generation of power and current.

During PV generate power, the power generation that PV is generating has changed with changing weather (temperature and irradiance), use MPP to monitor the new peak power produced as a result of the change. If the MPPT is slow in finding the peak power, the power losses are high, and vice versa. A good MPPT is needed to collect the power that the PV cell can generate.

4. DC-DC Converters

A DC-DC converter is a type of power transformer that is an electronic circuit, by temporarily storing input energy and then releasing that power to the output but with different voltages, converts a direct current (DC) power source from one voltage level to another. By using the characteristic of Magnetic fields in (inductors, transformers) or electric field storage elements may be contained in any of the storage components (capacitors) [4].

The output power and input power can be controlled by controlling the duty cycle (ratio of turn on/off time) between the input and output. The benefit of duty cycle uses to control output voltage, the input current, the current of the output, or to maintain constant power. Isolation between the input and output can be provided by transformer-based converters. For certain topologies, the key disadvantages of switching converters include difficulty, electronic noise, and high cost. In the literature, several different kinds of DC/DC power converters are suggested [2].

In this paper, the DC-DC converter used is boost which is using as step-up voltage(step-down current) the principle working is opposite to the buck converter, in the PV system using boost converter to increase the voltage to desire value that needed, the figre shows the circuit diagram of DC-DC boost converter [5].

It can represent the operation of boost converter by the equation (4).

$$V_{in}.t_{on} + (V_{in} - V_0).t_{off} = 0 \qquad (4)$$

V_0 = the output voltage

V_{in} = input Voltage

t_{on} = the peride time on

t_{off} = the peride time off

From equation (4) it can show the effect of duty cycle on the output voltage :

$$\frac{Vin}{V_0} = \frac{t_{on}+t_{off}}{t_{on}} \qquad (5)$$

From equation (5) $T = t_{on} + t_{off}$, T is the period of the switch, the duty cycle is calculated by the ratio of T and t_{on} . so we can control the output voltage very easily by the control duty cycle.

5. Maximum Power Point Tracking Algorithms

Maximum Power Point Tracking (MPPT) is a photovoltaic (PV) transducer algorithm that continuously modifies the impedance seen by the solar array to preserve the variable efficiency of the PV device at the peak power of the PV panel. Conditions, such as sunshine, temperature, and battery alterations [2].

MPPT algorithms are implemented by engineers designing solar inverters to optimize the power produced from photovoltaic systems. Algorithms regulate voltage to ensure that the device runs on the power voltage curve at the "maximum power point" (or maximum voltage), figure (6)shows how MPP change with changing irradiance [7].

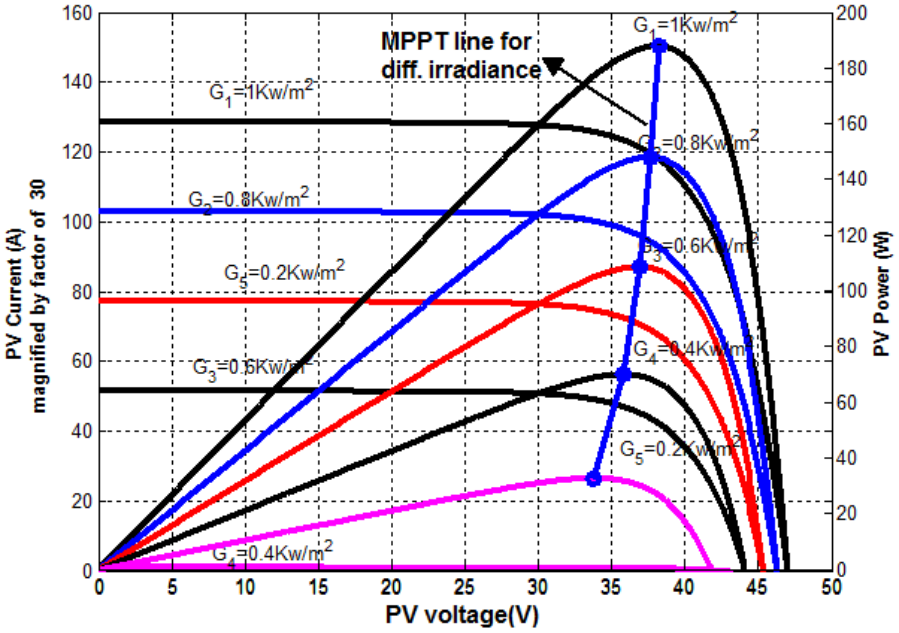

Figure 6: changing MPP with changing irradiance [11]

For PV systems, MPPT algorithms are widely used in controller design. In order to ensure optimum photovoltaic device power generation at all times, these algorithms take into account variables such as variable radiation and temperature.

In this paper most popular MPPT algorithms are discussing which is P&O and INC:

5.1. Perturbation and Observation P&O Algorithm

Perturb and Observation is one of the conventional methods to find MPPT and the most popular method, in P&O to calculate the MPP randomly choosing a point then makes incremental changes to the voltage and monitors changes in power. Figure (7) shows operation of P&O algorithm, if the change in voltage increase the power output of the solar panel the next perturbation will be in the same direction, if the change in the voltage decrease the power output of the panel then the next perturbation will be in the opposite direction. Till the difference between the previous power and new power equal to zero means ΔP is equal to zero, this point is MPP, but in P&O never stay even in best MPP because the Algorithm continuously searching the better power this is causing the oscillation around MPP and loss power and that's the biggest disadvantage of this method.

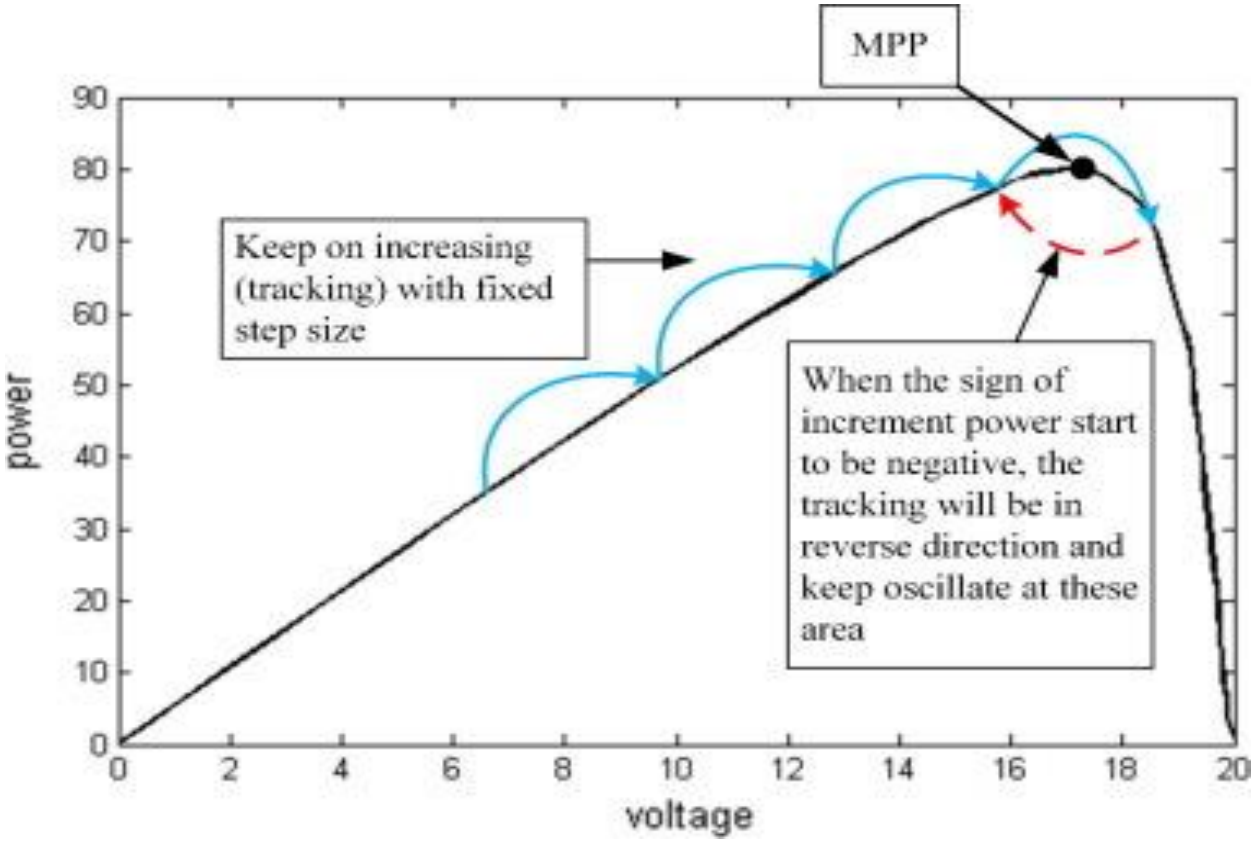

Figure 7: illustrate the operation of the P&O algorithm [12]

The table(1) shows all possibilities in the P&O algorithm. P&O have ability to find voltage V_{MPP} and current I_{MPP} automatically under change in weather condition (irradiance and temperature)for the PV panel or array [3].

Table 1. Shows all possibility in P&O algorithm

Prior perturbation	Change in power	Next perturbation
Positive	Positive	Positive
Positive	Negative	Negative
Negative	Positive	Negative
Negative	Negative	Positive

The following flowchat is illustrate the operation of P&O Algorithm

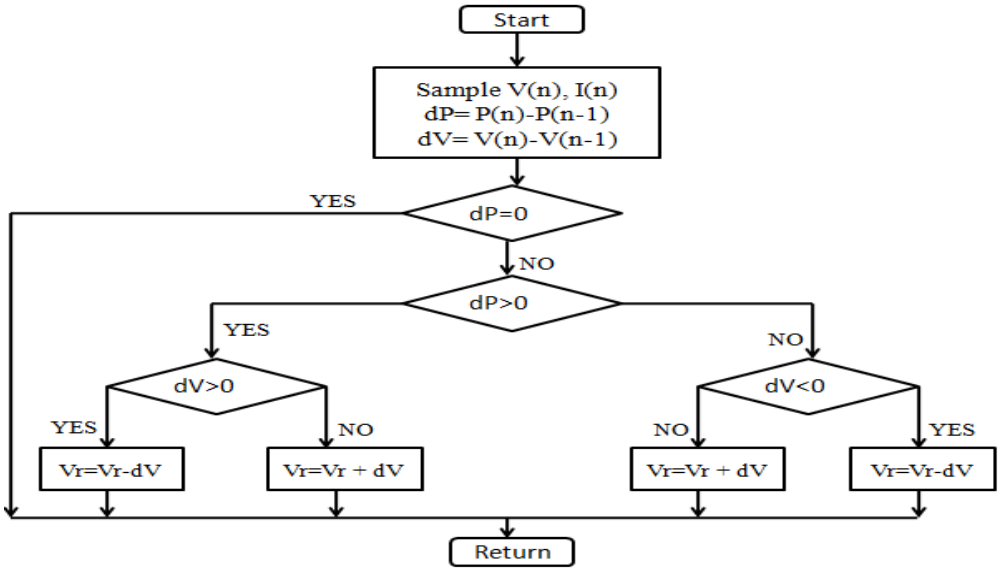

Figure 8: the flowchat of P&O algorithm [13]

5.2. Incremental and Conductance (INC) Algorithm

The incremental conductance method (INC) technique is one of the hill claim methods which is a direct technique, some of the drawbacks in P&O can be solved by using (INC) conductance like rapid change environmental. The basic idea of the incremental conduction (INC) method on the Ppv - Vpv curve of the PV module. The slope of the PV curve is zero at MPP, it decreases to the right of MPP and increases on the left side of MPP and this is shown in Figure (9).

The MPP in the PV module occurs when $\frac{dP}{dV} = 0$ and

$\frac{dP}{dV} > 0$ then $V_P < V_{mpp}$ at left of MPP

$\frac{dP}{dV} = 0$ then $V_P = V_{mpp}$ at the MPP

$\frac{dP}{dV} < 0$ then $V_P > V_{mpp}$ at right of MPP

From the description above we can write equation (6):

$$\frac{dP}{dV} = \frac{d(V.I)}{dV} = I\frac{dV}{dP} + V\frac{dI}{dV} \qquad (6)$$

$$= I + V\frac{dI}{dV}$$

Also, the MPP can be found by the ratio of changing current and voltage:

$\frac{\Delta I}{\Delta V} > -\frac{1}{V}$ then, at left of MPP

$\frac{\Delta I}{\Delta V} = -\frac{1}{V}$ then, at the MPP

$\frac{\Delta I}{\Delta V} < -\frac{1}{V}$ then, at right of MPP

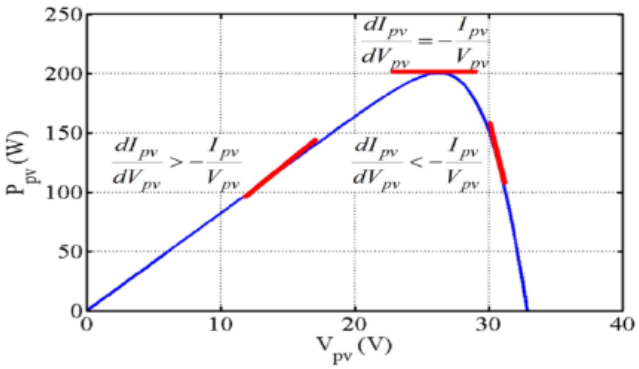

Figure 9: the flowchat of INC algorithm

The operation of incremental conductance can be illustrated by the following flowchart.

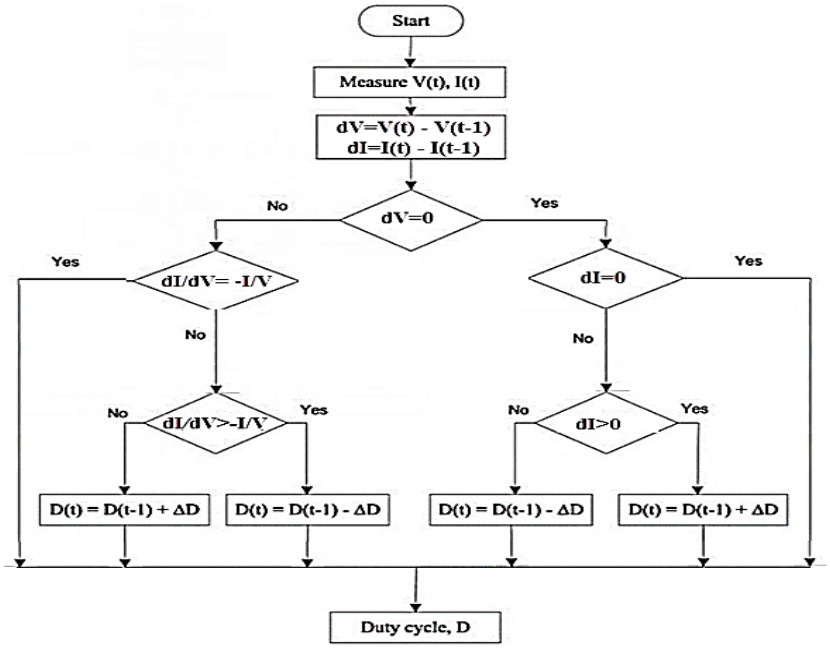

Figure 10: the flowchat of INC algorithm [14]

5.3. Hill Claim

As previously mentioned Maximum power point tracking used to extract the maximum power that the PV module can generate when the weather is changing, for this application, the Hill Claim algorithm uses a charge controller. At a certain point, the current and voltage can generate the maximum PowerPoint. This point (MPPT) is changed when the weather changes which are Irradiance and temperature. Hill Claim algorithms Use on a large scale in the PV systems in the process because of their simplicity and it does not require a study or source modeling features and can explain the properties of the drift because of the statute of limitations and shading other operational irregularities [9].

The basic operation of this algorithm first memorized the previous value of current I (k-1) and voltage V (k-1) for voltage and current and then calculate the power P (k-1). Then calculate the strength of P (k) current from the current-voltage and current. If the power is greater than the previous value, then the next step goes forward, and if the next step is less than the previous power, then maybe the maximum power point (MPP) or (local maximum) as shown in Figure(11.B) This is biggest a drawback to this algorithm. So it is normal for the power output in this way to be smaller than the other method. The operation of hill climb algorithm can be shown by the flowchat in Figure (11.A).

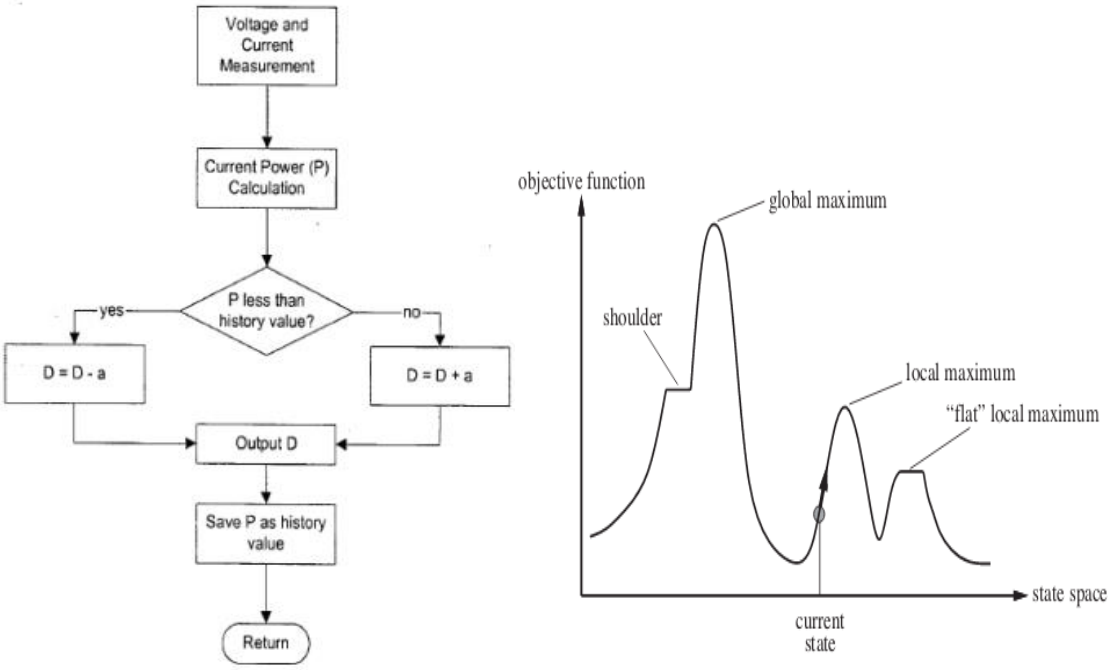

Figure 11:

A) Flowchart of the hill-climbing algorithm. B) State Space diagram for Hill Climbing

6. Linear and non-Linear load

Depending on how they draw current from the main power supply waveform, electrical loads can be are classified as linear or non-linear loads.

In terms of Linear loads, the voltage and current waveforms are sinusoidal, and the current is proportional to the voltage at all times (Ohm's law). However, in a DC system, a Linear load is a purely resistive load in which there is a linear relationship between the values of Current and Voltage. Most of the conventional lighting systems are accounting for linear loads [9].

Regarding non-linear loads, on the other hand, the current is not proportional to the voltage and fluctuates according to the alternating load impedance. Non-linear loads are usually connected to the electrical source via electronic devices. This means there will be a non-linear relationship between the values of the voltage and current. All capacitive, inductive, and motors are accounting for non-linear loads.

7. Simulation and design:

In this article simulation PV array working in a stand-alone system, PV system doesn't connect to the grid because the MPPT algorithm operation is identical, since MPPT control works through DC/DC converter. Therefore, an inverter is not required and only a DC/DC converter is connected between the PV array and the load. The PV system model used in Simulink can be seen in Figure (10).

In all PV systems, two inputs to the PV array variable which is are irradiance and temperature. These values temperature and irradiance in the daytime changing between 50 to 500, 200 to 1000 W/m2 respectively. Then, the PV array model consists of 9 Parallel strings and 17 Series-connected modules per string.

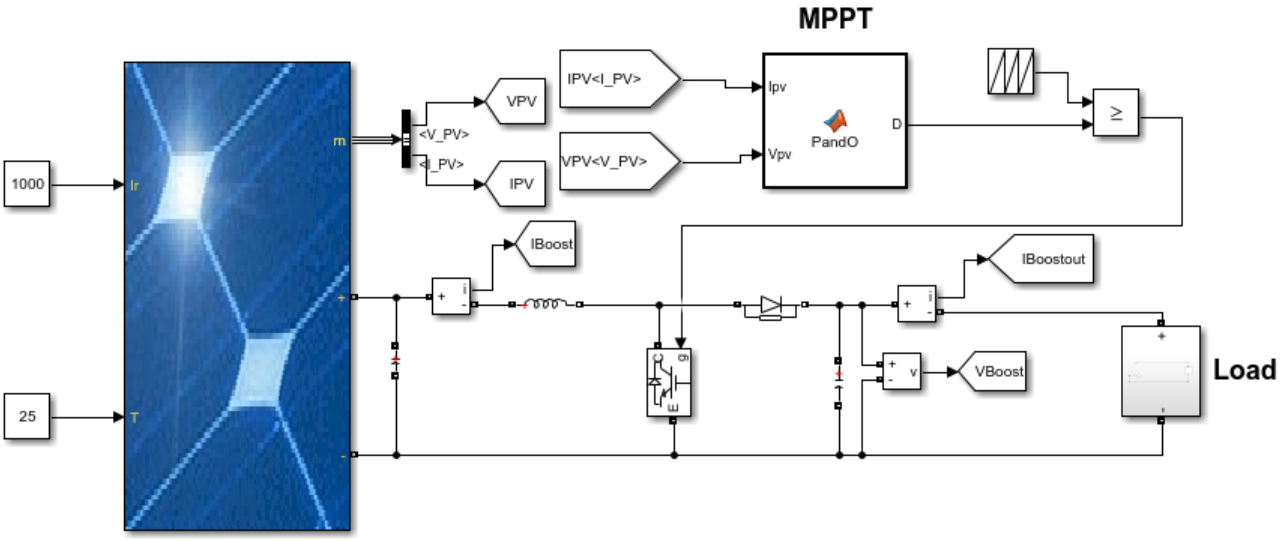

Figure 12: MATLAB Simulink Model PV System

- $I_{sc} = 7.97$ A
- $V_{oc} = 36.6$ V
- $I_{mpp} = 7.47$ A
- $V_{mpp} = 29.3$ V
- $P_{mpp} = 33.49$ kW

The value compound DC-DC Boost converter used in the model.

(L = 4.5 mH),
(C = 5000 μF)

(LC) functions as a low pass filter.

The MPPT algorithm will control duty ratio (D) and thus PV voltage (Vpv) in this converter. Furthermore, the DC battery maintains a constant voltage that must be maintained unless the MPPT algorithm changes the converter's duty ratio (D). In this converter, the MPPT algorithm to control the PV power (P_{pv}) working in maximum voltage and current point it should MPPT can control the duty ratio (D). The DC battery generates a constant voltage that must remain constant unless the MPPT algorithm changes the operating ratio converter (D).

In the end, the MPPT algorithm model block comprises. The MPPT use the voltage (Vpv) and current (Ipv) of PV are used as inputs, which are altered by a low pass filter to obtain true signal values free of noise. As a result, D is obtained and updated to the converter after their review.

8. Results and discussion:

In this part, The results of simulating for all algorithm methods are shown, first of all, the effect of variation solar irradiance, in the second part, the effect of changing temperature is discussed. This article focused on the power input and output power for both linear and non-linear load because the power is a result of voltage and current. all the figures collected the power of PV and output power for the linear and non-linear load to illustrate the comparison.

**** Note: Because the load for linear (resistor) and non-linear (DC-Motor) loads is constant in all cases, the effect of different MPPTs on output power simulation is very clear.***

8.1. Under Variable Solar Irradiance

8.1.3. P&O Algorithm

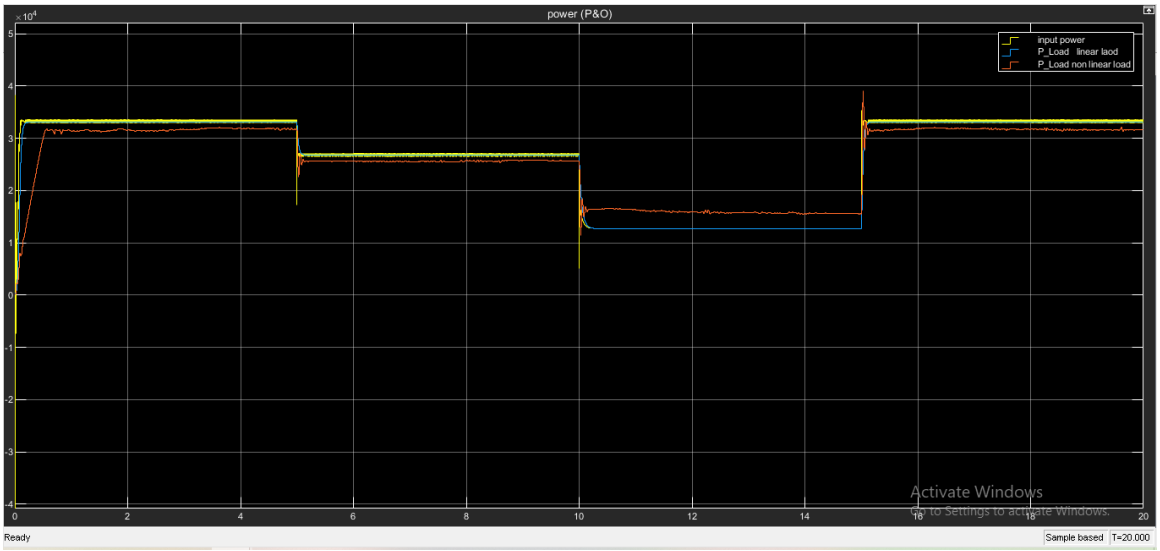

Figure 13: The output powers for perturb & Observation (P&O) under changing irradiance (1000, 800, 500, 1000)

Figure (13) shows the results of the power P&O algorithm under changing temperature from (1000,800,500,1000) W/m2, the yellow line shows the power input with more oscillation compare to the blue line which is the power of linear load, but in non-linear load (DC Motor) the output power is lower with more oscillation. For the non-linear load (DC Motor) witch shows the time need to get a steady-state is very high compare to the power linear load. The power generation by PV in both linear and non-linear loads is nearly the same. Because we have different loads, the output power level is very different. Also, the non-linear load affected the power generation and made the oscillation was high.

For each irradiance changing the P&O could find MPPT that is mean the algorithm working properly.

The rising time of the P&O Algorithm needed to reach the steady-state is smaller than INC Algorithm, but the oscillation of P&O is greater than INC Algorithm.

8.2.1. Hill Climbing (HC) Algorithm

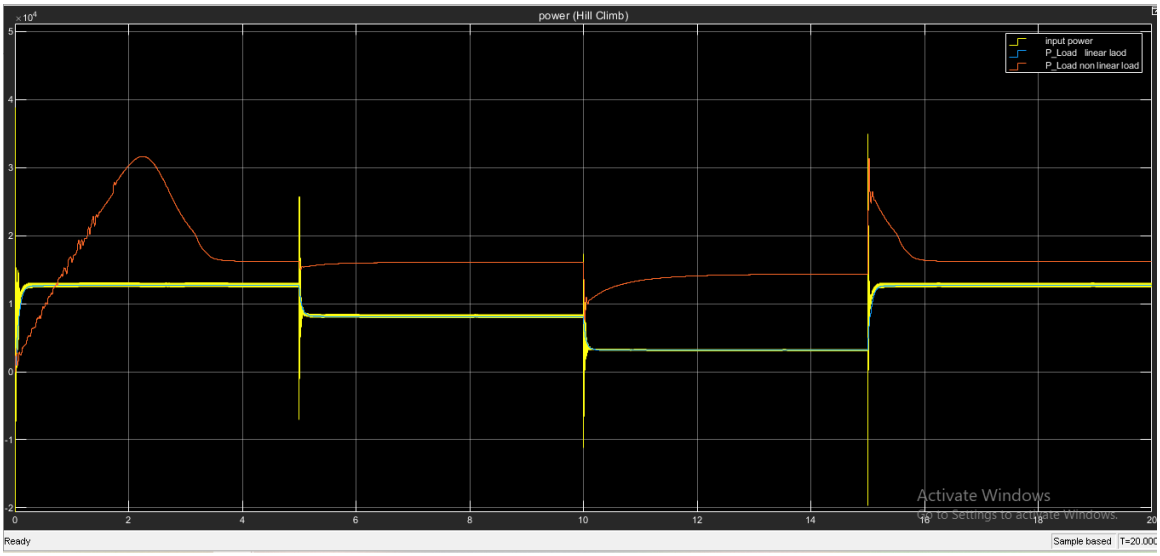

Figure 14: The output powers for Hill Climbing (HC) under changing irradiance (1000, 800, 500, 1000)

In Hill Climb (HC) algorithm opposite to P&O, INC algorithm the output power of the PV is very low as mentioned before for HC algorithm, it is normal because it cannot find the best power that the panel can generate. Also, we note that the time needed to rich steady state for non-linear load is more than the linear load.

8.1.3. INC Algorithm

In the case of a sudden shift in solar irradiance, the INC algorithm takes longer to hit the new MPP in non-linear load, as shown in Figure (14). As a result, the system's performance under variable solar irradiance is poor.

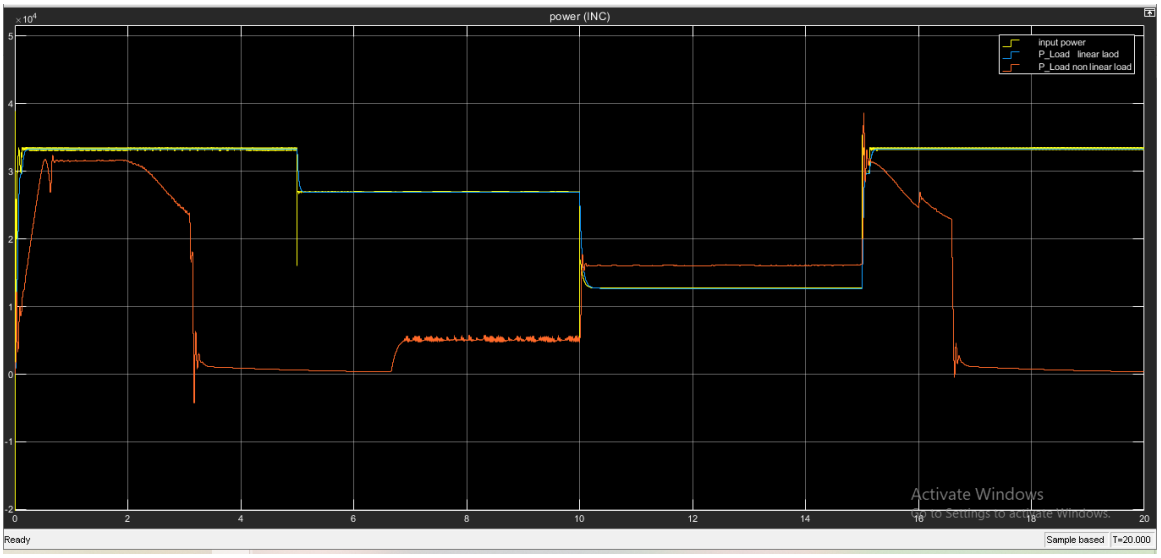

Figure 15: The output powers for Incremental Conductance (INC) under changing irradiance (1000, 800, 500, 1000)

The three figures(13,14,15) shows the effect of changing irradiance on power generation and output power for a linear and non-linear load like all the case the oscillation in non-linear load is high and affect of change irradiance is very clear in non-linear load the rising time needed to saturation is higher than non-linear.

In general, when irradiance change directly affected output power, P&O is better than the two other algorithms in order to reach steady-state, oscillation and output power for the linear and non-linear load.

8.2. Under variable solar temperature

8.2.1. P&O Algorithm

The Figure (16) shows the effect of variable temperature Change in temperature (25, 35, 45, 25) at 0, 5, 10, 15.

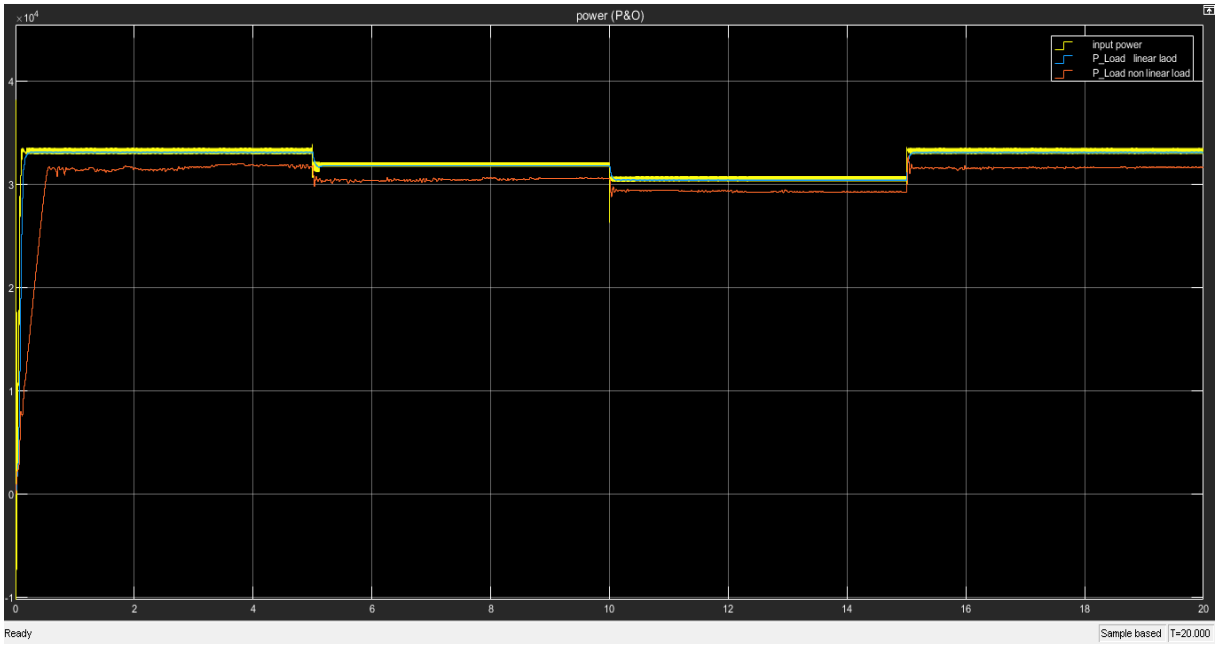

Figure 16: The powers output for P&O algorithm under variable temperature after (25, 35, 45, 25) at 0, 5, 10, 15 seconds, respectively.

In the P&O algorithm for changing temperature the output power is changing, the algorithm can find the MPPT in all cases of changing temperature. But in non-linear load, the oscillation is higher than the linear load. Also, the rising time is greater than the linear load.

8.2.2. Hill Climb (HC) Algorithm

The Figure 17), shows the effect of variable temperature on the output power for linear and non-linear load.

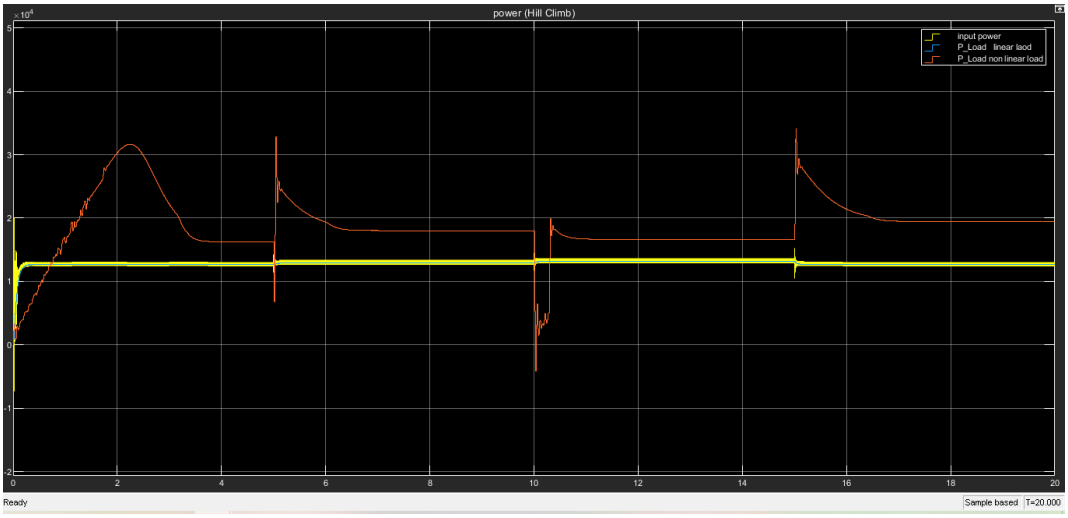

Figure 17: The powers output for Hill Climbing (HC) algorithm under variable temperature after 5 seconds (25, 35, 45, 25)

The change in temperature shows that in P&O and INC the time needed to saturate is very small compared to the HC algorithm. In HC algorithm for changing temperature the output power is changing, the algorithm cannot find the MPPT any case of changing temperature. In non-linear load the oscillation is higher than the linear load. Also, the rising time is greater than the linear load.

8.2.3. Incremental Conductance (INC) Algorithm

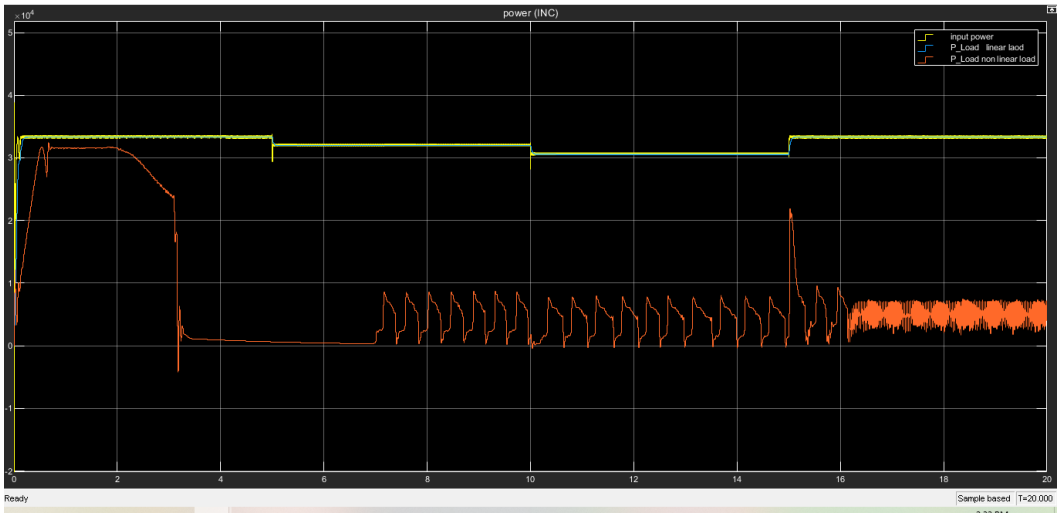

Figure 18: The powers output for Hill Climbing (HC) algorithm under variable temperature after 5 seconds (25, 35, 45, 25)

Figure (18) shows the power of nonlinear load has a very large oscillation. The INC algorithm has the ability to find MPPT when the temperature is changing in all cases.

9. Conclution

In this article to compare the effect of linear and non-linear load The two most popular MPPT algorithms, P&O, HC, and INC, those algorithms were selected their performance and dynamic MPPT efficiencies were examined. Both (P&O, INC) algorithms could find the MPP properly, but Hill Climb (HC) algorithm mostly couldn't find the actual MPPT because of their property described above.

The effect of linear load and nonlinear load on PV power and output power is shown. oscillation in output power and the rising time to MPPT is a large difference. in the simulation, it can notice that all algorithms have the advantage and disadvantage. The load connected to the output is not the same so it can not compare the power between linear load and non-linear load very well.

10. References

[1] G. P. G. S. M. V. N. Femia, "Optimizing sampling rate of P&O MPPT," *in Proc. IEEE PESC,* pp. 1945- 1949, 2004.

[2] L.-W. L. Huang-Jen Chiu, "A Bidirectional DC–DC Converter for Fuel Cell Electric Vehicle Driving System," *IEEE TRANSACTIONS ON POWER ELECTRONICS,* Vols. VOL. 21, NO. 4, pp. 950-959, JULY 2006.

[3] B. U. S. V. D. D. P. Jacob James Nedumgatt, "Perturb and Observe MPPT Algorithm for PV Systems-Modeling and Simulation," *researchgate,* December 2011.

[4] High Step-Up Gain DC-DC Converter with Switched Capacitor and Regenerative Boost Configuration for Solar PV Applications.

[5] Analysis of DC/DC Boost Converters Design Methods Dr. Stephan Bayne 2015.

[6] Freris, L. and D. Infield, Renewable energy in power systems. 2008: John Wiley & Sons..

[7] Boost Converter Design and Analysis for Photovoltaic Systems YavuzBahadır KOCA1– Yılmaz ASLAN2 – Ahmet YÖNETKEN3 – Yüksel OĞUZ4,*.

[8] CCM and DCM operation of the integrated-magnetic interleaved two-phase boost converter.

[9] DESIGN, SIMULATION AND IMPLEMENTATION OF A HIGH STEP-UP Arash torkan 2016.

[10] Boost Converter Design and Analysis for Photovoltaic Systems.

[11] Mechanical Sun-Tracking Technique Implemented for Maximum Power Point Tracking of a PV System for Effective Energy Supply - Scientific Figure on ResearchGate. Available from: https://www.researchgate.net/figure/MPPT-at-different-irradiance-for-I-V-P-V-of-PV-panel-at-constant-temp-of-25-o-C_fig1_285400008

[12] Awang JUSOH, Rozana ALIK, Tan Kar GUAN, Tole SUTIKNO "MPPT for PV System Based on Variable Step Size P&O Algorithm" TELKOMNIKA, Vols. VOL. 15, NO. 1, p.84 , MARCH 2017.

[13] Design of Hybrid Solar Wind Energy System in a Microgrid with MPPT Techiques - Scientific Figure on ResearchGate. Available from: https://www.researchgate.net/figure/Flowchart-of-P-O-MPPT-algorithm_fig1_323720840

[14] PSIM and MATLAB Co-Simulation of Photovoltaic System using “P and O” and “Incremental Conductance” MPPT - Scientific Figure on ResearchGate. Available from: https://www.researchgate.net/figure/flowchart-of-Incremental-Conductance-algorithm_fig5_307598655

INTERNATIONAL JOURNAL OF ELECTRONICS, MECHANICAL AND MECHATRONICS ENGINEERING
Vol.10 Num.1 - 2020 (1785-1794)

Received: 19.10.2019
Accepted: 02.12.2019

PV Panel Based Micro Inverter Using Boost Control Topology with PWM and MPPT (Perturb and Observe) Method

Mir Alam KHAN[1], Prof. Dr. Mehmet Emin TACER[2]

Abstract - Over the past years, the energy demand has been steadily growing and so methods of how to cope with this staggering increase are being researched and utilized. One method of injecting more energy to the grid is renewable energy, which has become in recent years an integral part of any country's power generation plan. Thus, it is a necessity to enhance renewable energy resources and maximize their grid utilization, so that these resources can step up and reduce the over dependency of global energy production on depleting energy resources.

This paper focuses on solar power and effective means to enhance its efficiency using different controllers. In this regard, substantial research efforts have been done. However, due to the current market and technological development, more options are made available that can boast the efficiency and utilization of renewables in the power mix.

In this paper, an enhanced maximum power point tracking (MPPT) controller has been designed as part of a Photovoltaic (PV) system to generate maximum power to satisfy load demand. The PV system is designed and simulated using MATLAB (consisting of a solar panel array, MPPT controller, boost converter, and a resistive load). New electrical codes require rapid solar system shutdown so first responders or firefighters are safe from high voltage when they need to be on rooftops or servicing power lines. Microinverters comply with these rapid shutdown requirements and have this capability embedded into each module. Each controller will be tested under two different scenarios; the first is when the panel array is subjected to constant amount of solar irradiance along with a constant atmospheric temperature and the second scenario has varying solar irradiance and atmospheric temperature. The performance of these controllers is analyzed and compared in terms of the output power efficiency, system dynamic response and finally the oscillations behavior.

Microinverters and the add-on optimizers have the ability to track the production of each individual panel, while with a standard inverter you only can track the production of the whole system. If you were to expand your system in the future, microinverters are simple to add one at a time. Each panel and microinverter pair can be easily added to your existing solar array without needing to worry about purchasing, siting, and installing additional string inverters.

Keywords: *Maximum Power Point Tracking, Perturb and Observe, DC-DC Converters, Photovoltaic System.*

[1] *Electrical Electronics Engineering, Engineering Faculty, Istanbul Aydin University, Istanbul, Turkey*
[2] *Electrical Electronics Engineering, Engineering Faculty, Istanbul Aydin University, Istanbul, Turkey, emintacer@aydin.edu.tr, ORCID: 0000-0001-8103-8470*
DOI: 10.17932/IAU.IJEMME.2010.001/ijemme_v10i1002

1. Introduction

In today's modern life solar panels and microinverters play a pivotal role. They are user friendly as well as environmentally friendly. They can be installed from a single house to number of cities. Photovoltaic system can be either stand-alone or connected to utility grid. The disadvantage of this PV generation depends on atmospheric conditions such as solar irradiance and temperature. Maximum power point trackers (MPPTs) play an important role in photovoltaic (PV) power systems because it is maximizing the output power of a PV system for a given atmospheric conditions. MPPT is maintaining operating point at the maximum power point using a different MPPT algorithm. MPPT can minimize the overall photovoltaic (PV) system cost. To maximize the output of a PV system, continuously tracking the maximum power point (MPP) is necessary.
This paper is organized as follows: First, it will discuss about our main circuit its configuration and working. Second portion will discuss about control scheme and how it will control our output voltage. In the third portion we shall discuss graphs at different irradiance and loads. And at the end conclusion and future work.

2. Principle

According to the theory of maximum power transfer, the power delivered from source to the load is maximum when the source internal impedance matches with the load impedance.

$$Z_S = Z_L$$

So, the impedance from the converter side needs to match the internal impedance of the solar array [2]. At that time the operating point is at the Maximum power point (MPP) so maximum power is obtained from the photovoltaic array.

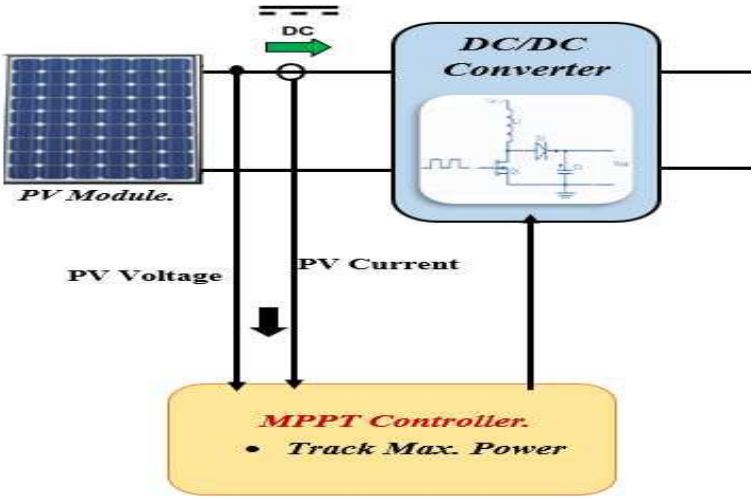

Fig. 1. Block diagram of Solar system using MPPT

3. Perturb and Observe (P&O)

The P&O algorithm uses simple feedback arrangement and little measured parameters. In this approach, the module voltage is periodically given a perturbation and the corresponding output power is compared with that at the previous perturbing cycle [12]. In this algorithm a slight perturbation is introduced to the system. This perturbation causes the power of the solar module varies. If the power increases due to the perturbation, then the perturbation is continued in the same direction. After the peak power is reached the power at the MPP is zero and next instant decreases and hence after that the perturbation reverses.
When the stable condition is arrived, the algorithm oscillates around the peak power point. In order to maintain the power variation small, the perturbation size is remained very small. The technique is advanced in such a style that it sets a reference voltage of the module corresponding to the peak voltage of the module.

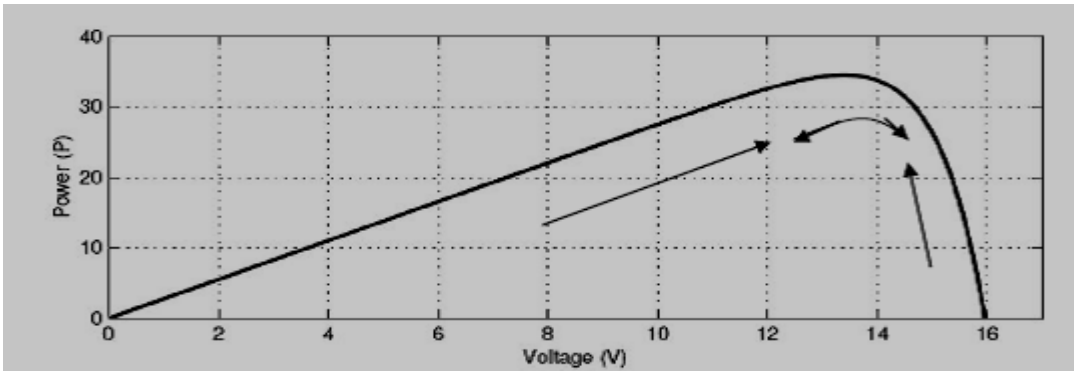

Fig. 2. Graph Power versus Voltage for Perturb and Observe Algorithm

4. Control Scheme:

As previously mentioned, this is one of the simplest methods to implement and only requires a voltage and current sensor to calculate the power and compare it to the previous cycle power. First, power is calculated using voltage and current and then compared to the previous value of the power. If the difference is equal to zero, then the same voltage will be returned, and the algorithm will try to oscillate around the same MPPT. If there is a change in power, the algorithm will then go forward and check the difference in voltage levels. In the case of a positive power difference, the algorithm will notice and direct the voltage to the same direction (increase or decrease) as the previous case. Hence, if the voltage difference is positive then the algorithm will keep increasing the voltage and vice versa. However, in the case of negative power difference, the algorithm will do the complete opposite and will direct the voltage to the other direction. This means that if the voltage change is negative then the algorithm will increase the voltage and finally if the change in voltage is positive the algorithm will decrease the voltage. Thus, the four cases that the algorithm is required to evaluate and react to are as follows:

1. $\Delta P > 0$ and $\Delta V > 0$ Increase the voltage.
2. $\Delta P > 0$ and $\Delta V < 0$ Decrease the voltage.
3. $\Delta P < 0$ and $\Delta V > 0$ Decrease the voltage.
4. $\Delta P < 0$ and $\Delta V < 0$ Increase the voltage.

The algorithm can manipulate the operating voltage freely by varying the duty cycle ratio. Any change in the duty cycle will consequently have an inverse effect on the input resistance of the DC/DC converter and thus will alter the operating voltage to satisfy the four cases mentioned above [5]. Table 1 illustrates the relationship between the duty cycle, input resistance, output power, and the voltage in the next cycle as shown below.

Table 1. Effect of Duty Cycle on Input Resistance, Output Power, and the Next Cycle's Voltage

Change in Duty Cycle	Change in Input Resistance	Effect on Output Power	Next Cycle's Voltage Change
Increase	Decrease	Increase	Decrease
Increase	Decrease	Decrease	Increase
Decrease	Increase	Increase	Increase
Decrease	Increase	Decrease	Decrease

As shown in Table 1, any change in the duty cycle will have an inverse effect on the input resistance of the converter and hence have an inverse effect on the operating voltage. The algorithm then observes the effect of that change in the duty cycle on the output power to calculate the right command in the next cycle. The output power can increase or decrease depending on whether the current operating voltage level is before or after the knee point in the power graph as shown in Figure 2. If the operating level is beyond the knee point or the MPP,

then an increase in the voltage will decrease the output power and vice versa. For example, in the third case in Table 1, a decrease in the duty cycle causes an increase in input resistance or operating voltage and results in an increase in the output power. This means that the current operating level is before the MPP and by increasing the voltage the output power will increase and thus in the next duty cycle the algorithm will opt to increase the voltage which can be achieved by reducing the duty cycle.

5. System Architecture

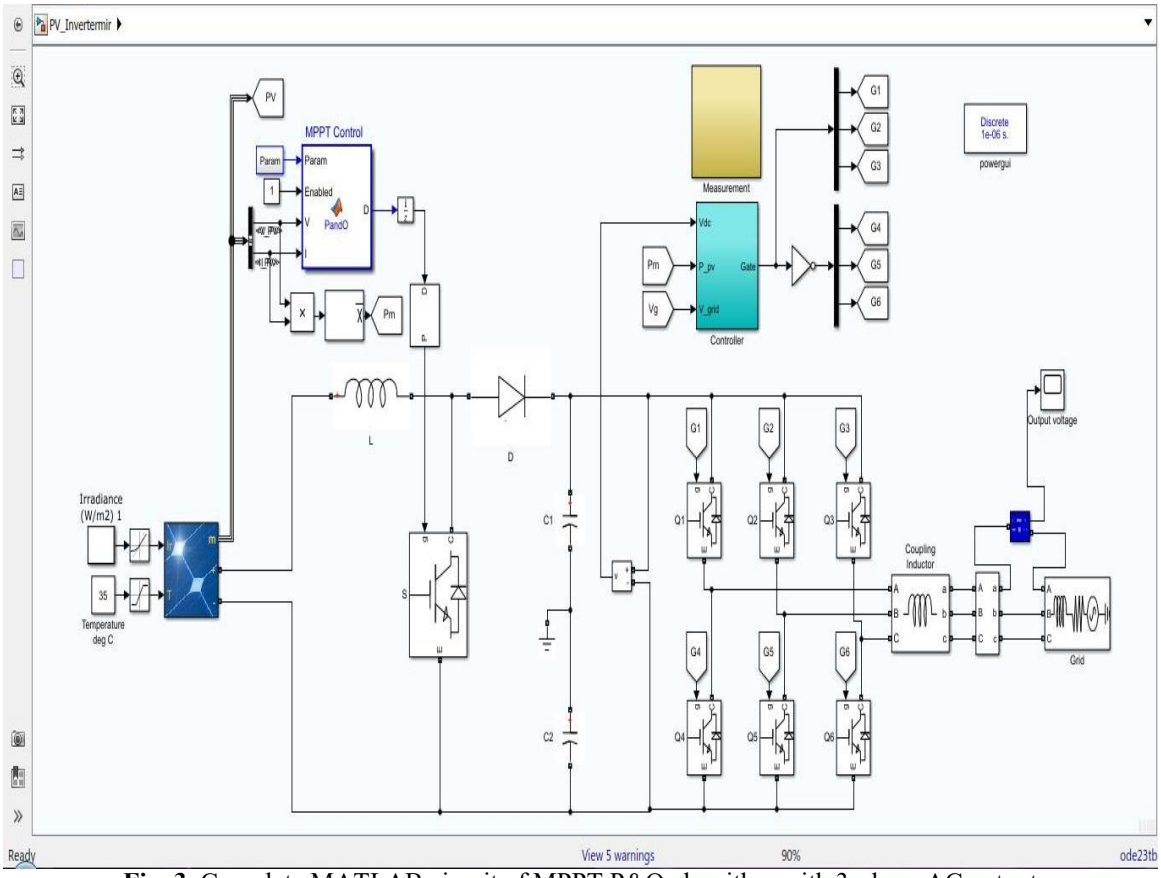

Fig. 3. Complete MATLAB circuit of MPPT P&O algorithm with 3-phase AC output

The modules in a PV system can be wired in series or in parallel depending on the output or power required. Wiring them in series increases the voltage while wiring them in parallel increases the current. The power, voltage, and current values are utilized to calculate the number of modules to be connected in series in a string and how many parallel strings are needed to reach the targeted output power. Therefore, the design has to have six modules connected in series in a string and 57 parallel strings to reach the required output power, which is 150 kW.

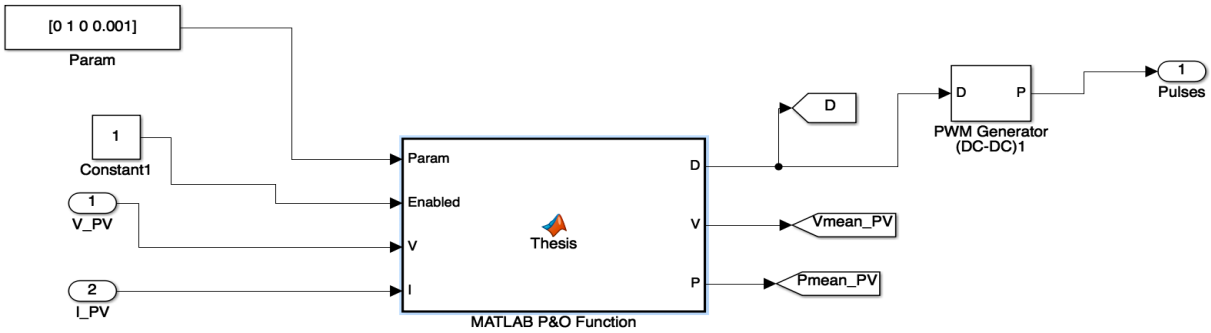

Fig. 4. Simulink/MATLAB P&O Function

In the first scenario, the solar panel will be subjected to a constant solar irradiance of 1000 W per square meter and will have a constant internal temperature of 25 ℃ as shown in Figure 5. This allows for a simple and reliable comparison of the algorithms' performance in terms of accuracy and speed to get the desired power output, which is 150 kW.

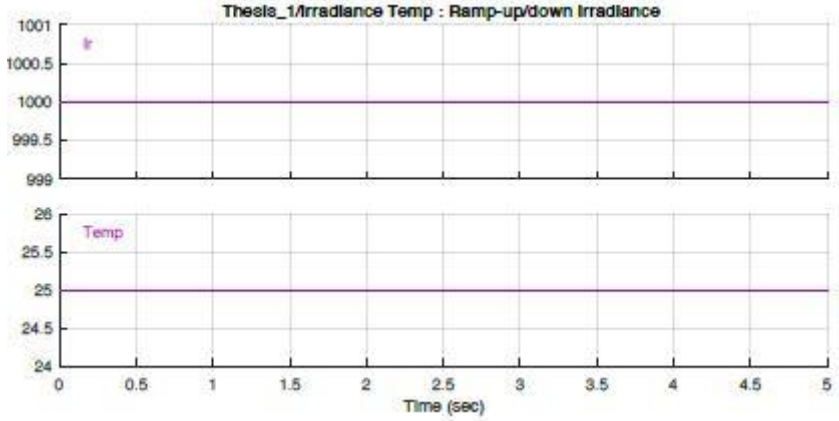

Fig. 5. Constant Irradiance and Temperature Signals

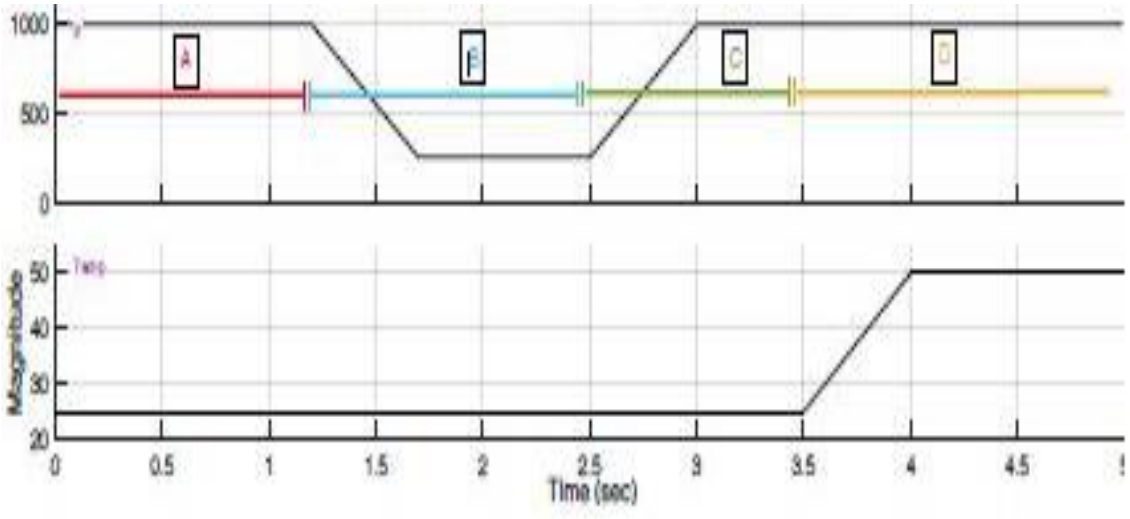

Fig. 6. Varying Irradiance and Temperature Signals

Table 2. Comparison Between the Four Periods in the Design

Period	Color Code	Irradiance Value (W/m^2)	Temperature Value (℃)	Time range (Sec)
A	Red	1000	25	0 – 1.2
B	Blue	250 ≤ IV < 1000	25	1.2 – 2.5
C	Green	250 < IV ≤ 1000	25	2.5 – 3.5
D	Yellow	1000	50	3.5 – 5

Scenario One: Constant Irradiance and Temperature

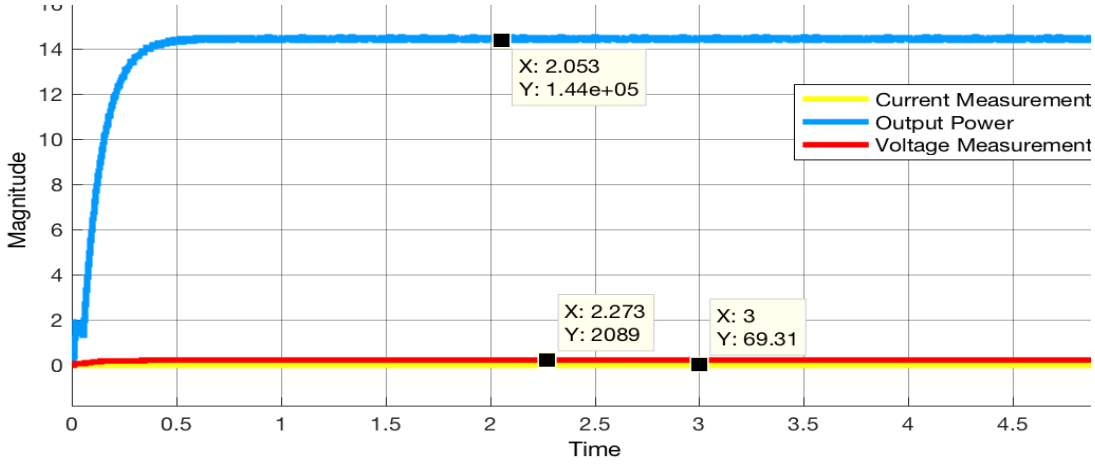

Fig. 7. Output Power Under Constant Conditions Using P&O MPPT

Using the P&O algorithm yields a fast response as expected where the rise time is about 0.197 seconds or approximately 0.2 seconds and the settling time is about 0.26seconds. The output power starts from zero and reaches a maximum value of 145,500W at time of 4.15 seconds.

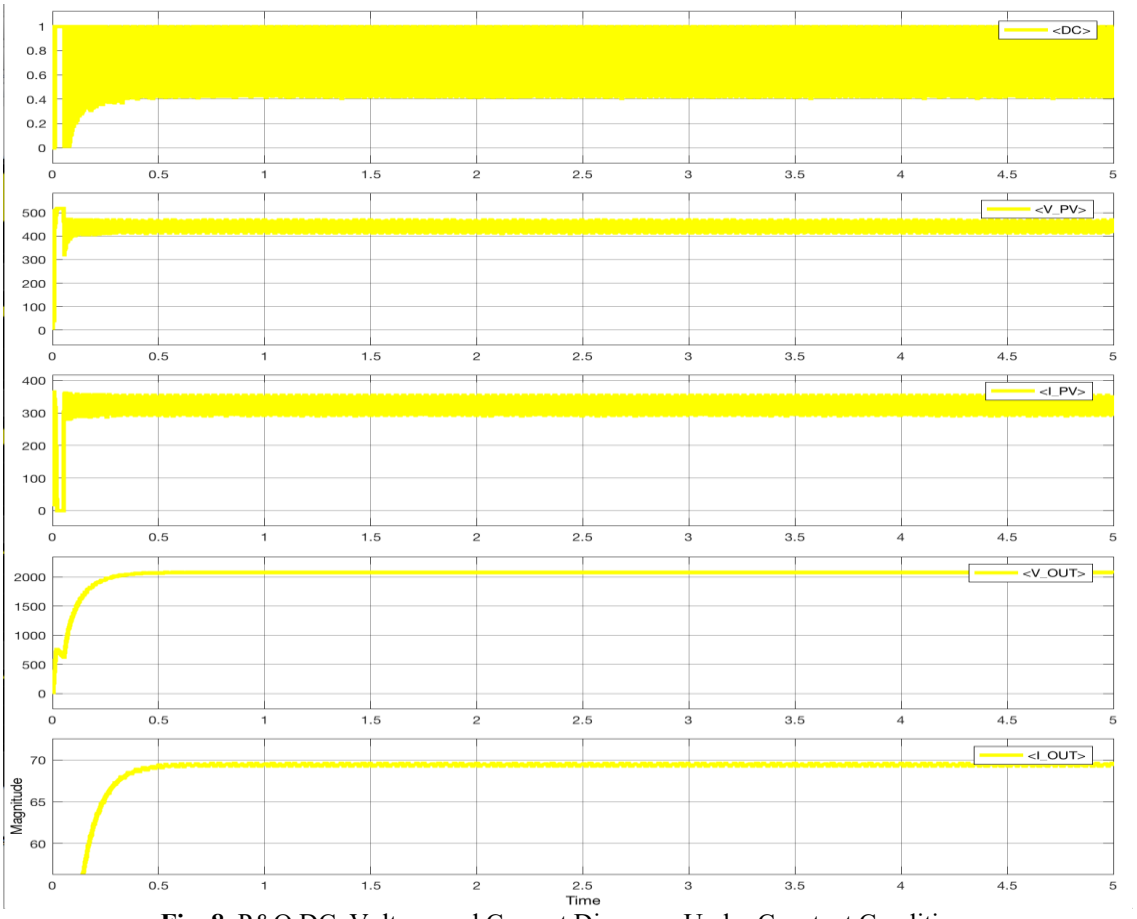

Fig. 8. P&O DC, Voltage and Current Diagrams Under Constant Conditions

Scenario Two: Varying Irradiance and Temperature

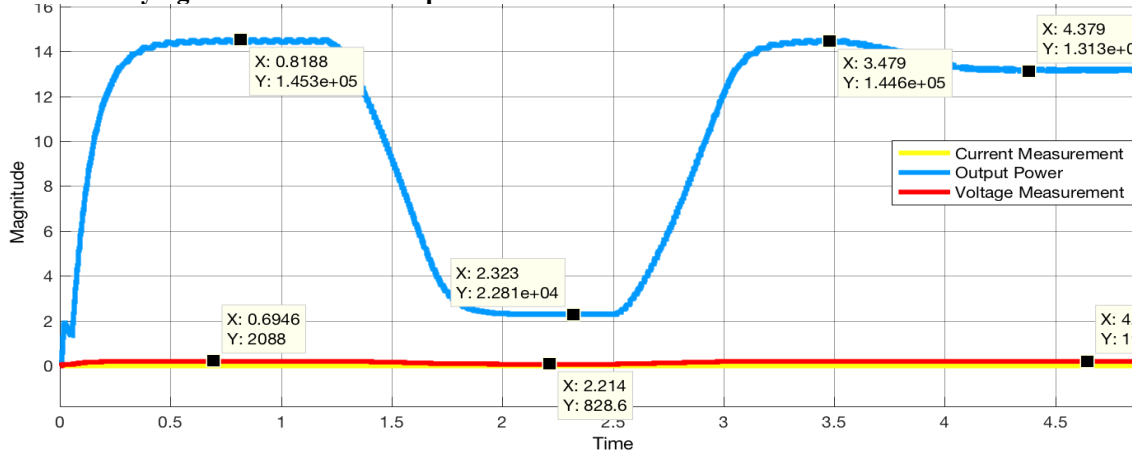

Fig. 9. Output Power Under Varying Conditions Using P&O MPPT

In fig. 9, period A has an irradiance of 1000 W per square meter and module temperature of 25 ℃ and has the output power curve increasing from zero to 144,700W of power. It drops down to about 22,990 W in period B when the irradiance is dropped to 250 W per square meter and the temperature is kept constant. In part C, the

irradiance is increased again to 1000 W per square meter and thus the power output is close to that in part A which is 144,400 W. Part C is done in preparation for part D, where the irradiance is kept constant at 1000 W per square meter and the temperature is increased from 25 to 50 ℃. This results in a power output drop from 144,400 W to 131,600W.

Table 3. P&O Efficiency Percentages of each Period

Period	Irradiance Value (W/m^2)	Temperature Value (℃)	Actual Output Power (W)	Theoretical Output Power (W)	Efficiency Percentage %
A	1000	25	144,700	150,600	96.08
B	250	25	22,900	36,460	62.81
C	1000	25	144,400	150,600	95.88
D	1000	50	131,600	135,300	97.27

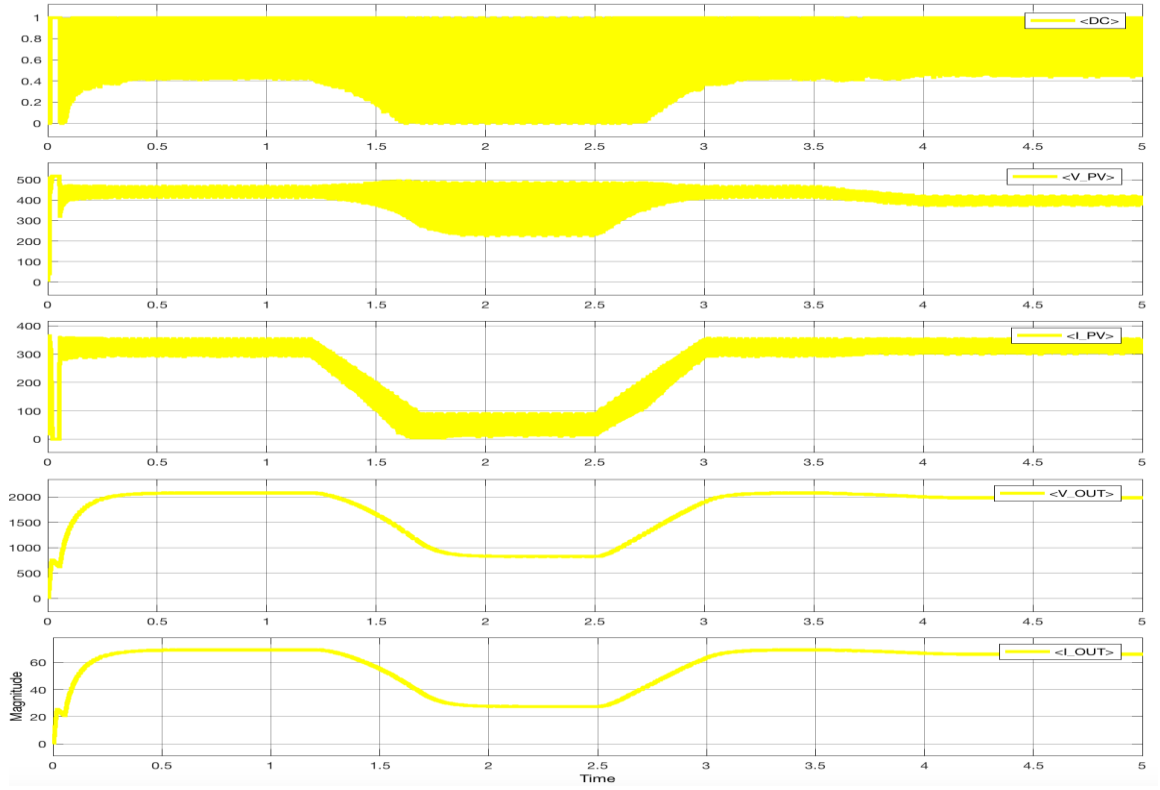

Fig. 10. P&O DC, Voltage and Current Diagrams Under Varying Conditions

The last part of this scenario (and section) is Fig. 10. This figure shows the duty cycle values, PV output voltage and current, and the system output voltage and current. Like the first scenario, the PV output voltage and current oscillate heavily until they pass through the boost converter, which allows for a boost in voltage, a drop in current, and removing the oscillations from both curves. Moreover, an observation in the PV voltage and current curves is that while a decrease in irradiance affects both these variables as shown in period B, the PV current is affected more.

The current drops from an average of 320 Amperes to an average of 80 Amperes, while the voltage only drops from an average of 450 Volts to about 350Volts. On the other hand, an increase in the temperature affects the PV voltage where it drops from 450 Volts to about 400 Volts; however, the temperature spike from 25 ℃ to 50 ℃ has an insignificant effect on the current that does not manifest on the curve. Finally, the voltage and current of the output system seem to react in a similar manner where they are both affected similarly during the drop in irradiance and rise in temperature. The output voltage starts at 2100 Volts in period A, drops to about 850 Volts in period B, goes back up to 2100 Volts in period C and finally reduces a bit more to 2000 Volts in period D. Likewise, the output current starts at 70 Amperes, drops to 28 Amperes, back to 68 Amperes, and finally reduces to about 66 Amperes.

6. Conclusion:

The core advantage of using microinverters is that theoretically, you can yield more solar electricity. The reason for this is that there are slight differences in currents between solar panels. When solar panels are in a string, the current is reduced to that of the least-producing panel in the string. P&O MPPT method is implemented with MATLAB-SIMULINK for simulation. The MPPT method simulated in this paper can improve the dynamic and steady state performance of the PV system simultaneously. Through simulation it is observed that the system completes the maximum power point tracking successfully despite of fluctuations. When the external environment changes suddenly the system can track the maximum power point quickly. Both buck and buck-boost converters have succeeded to track the MPP but, buck converter is much more effective especially in suppressing the oscillations produced due the use of P&O technique.

References

[1] A. e. a. Khamis, ""A review of islanding detection techniques for renewable distributed generation systems."," *Renewable and sustainable energy reviews,* pp. 483-493., 2013.

[2] S. K. Z. a. B. M.-I. Abapour, ""Evaluation of technical risks in distribution network along with distributed generation based on active management."," *IET Generation, Transmission & Distribution8.,* pp. 609-618., 4 (2013).

[3] "http://www.eere.energy.gov/RE/bio_resources.html," [Online].

[4] a. P. W. Quan Li, "A Review of the Single Phase Photovoltaic Module Integrated Converter Topologies with Three Different DC Link Configurations," *IEEE Transactions on Power Electronics,,* Vols. Vol. 23, , no. No. 3, pp.1320-1333., (2008) .

[5] e. a. s. b. kjaer, ""a review of single-phase grid-connected inverters for photovoltaic modules"," *ieee transactions on industrial application,* Vols. Vol. 41,, no. no. 5, , p. pp.1292–1306, sep. 2005.

[6] M. M. S.Sallem, "Energy management algorithm for an optimum," *control of a photovoltaic water pumping system, applied energy, , ,* vol. 86, pp. 2671- 2680, 2009.

[7] A. Betka and A. Moussi, "Performance Optimization of a Photovoltaic Induction Motor Pumping System,," *Renewable Energy,,* Vols. 29, pp. 2167-2181, 2004.

[8] A. M. A. B. N. T. A. Terki, "An improved efficiency of fuzzy logic control of PMBLDC for PV pumping system,," *Applied Mathematical Modeling,* Vols. 36, no.3, , pp. 934-944, 2012.

[9] A. M. A. B. N. T. A. Terki, "An improved efficiency of fuzzy logic control of PMBLDC for PV pumping system,," *Applied Mathematical Modeling, ,* Vols. 36, no.3, pp. 934-944, 2012.

[10] L. K. P. S. S. Sumathi, "Solar PV and Wind Energy Conversion Systems," 2015.

[11] E. O. A. B. a. A. L. V. Salas, "Review of the Maximum Power Point Tracking Algorithms for Stand-Alone

Photovoltaic Systems," *Solar Energy Materials & Solar Cells,* Vols. 90, pp. 1555 -1578, , 2006..

[12] R. D. Lalouni S, "Approch for maximum power point tracker of standalone PV system using fuzzy controller, in Proc.," *IREC 2011, Tunis, 20-22, ,* pp. I-6, 2011, .

[13] S. K. P. DEBASHIS DAS, "MODELING AND SIMULATION OF PV ARRAY WITH BOOST CONVERTER: AN OPEN LOOP STUDY," *NATIONAL INSTITUTE OF TECHNOLOGY,* pp. 15-25, 2011.

INTERNATIONAL JOURNAL OF ELECTRONICS, MECHANICAL AND MECHATRONICS ENGINEERING
Vol.10 Num.1 - 2020 (1795 - 1805)

Received: 18.11.2019
Accepted: 23.12.2019

Strengthening a Historical Building with Carbon Fiber Bands

Gülizar TAŞ[1], Sepanta NAİMİ[2], Mehmet Fatih ALTAN[3]

Abstract - In general, horizontal stresses that occur during earthquakes cause cracks in masonry walls. In old buildings, usually wooden or iron beams were used as tension members. These beams rotted on the walls of many old buildings examined and lost their tensile properties. This may be riskier, especially where there is more atmospheric pollution, and the increase in this pollution in the next centuries may result in these beams lasting 100 years or less instead of about 300 years. In this study, an exemplary historical building is modeled and analyzed in the SAP2000 program using finite element method, and a mixed system in which carbon fiber bands and carbon fiber meshes are used together is proposed to strengthen the masonry walls. Thus, we can say that these pull elements added to the structure are a system that acts as a stirrup that prevents the masonry walls from opening laterally.

Keywords: *Masonry Wall, Reinforcement, Seismic Performance, Beam, Carbon Fiber Material.*

1. Introduction

The main purpose of strengthening or improvement works is to increase both the ability of the structure to behave better in the case of inelastic deformation and to increase the load carrying capacity and integrity of the structure. One of the most commonly used methods for reinforcing masonry structures consists of applying externally bonded carbon fiber composite materials. The use of this material has become popular due to its lightweight and advantageous mechanical properties. However, the potential of carbon fiber

[1] *Department of Civil Engineering, Istanbul Aydin University, Istanbul, Turkey.*
[2] *Assoc., Prof., Dr., Department of Civil Engineering, Istanbul Aydin University, Turkey, e-mail: sepantanaimi@aydin.edu.tr, ORCID: 0000-0001-8641-7090*
[3] *Prof., Department of Civil Engineering, Istanbul Aydin University, Turkey, e-mail: mehmetaltan@aydin.edu.tr, ORCID: 0000-0003-0961-0115*
DOI: 10.17932/IAU.IJEMME.2010.001/ijemme_v10i1003

material reinforcement techniques is still far from fully utilized when applied to masonry structures due to compatibility issues. In this study, our subject is to make static analysis of a sample structure, to examine the horizontal and vertical load bearing systems, and also to create a mathematical model of the building using the finite element method. In order to determine the structural behavior in the most accurate way, the geometry of the building was largely complied with in modeling studies and modeled in three dimensions. The old pictures of the historical building were selected from engravings and modeled by adhering to the most appropriate building system.

2. Materials and Methods

The creation of the mathematical model of the building started with the creation of a 3D building model in the CAD environment as a result of the architectural studies. The information about the bearing elements and the data obtained from the ground study report were compiled and these collected data were processed on the prepared model. After defining the geometry of the structure in the CAD environment, the prepared geometric model was transferred to the SAP2000 program. The load-bearing walls are defined in the SAP2000 program with the help of solid and wooden roofs and 3 small domes with the help of surface elements. Wooden columns and beams used on the roof are included in the model with the help of frame elements. In modeling studies, it was aimed to divide finite elements into more parts in statically critical sections and to obtain more precise results in these regions [1]. During the finite element decomposition process, it is ensured that the nodal points where different elements intersect with each other are compatible with each other and do not create discontinuities.

In the next step, the boundary conditions, degrees of freedom of the supports and nodal points and the loads affecting the model were determined and entered in the SAP2000 environment in line with the determined geometric conditions of the structure, and thus the model was ready for analysis. In the analysis of the model, the geometrical and material non-linear behavior of the structure and the possibility that the mistakes that can be made may cause wrong results are not taken into account. As a result, the structure has been analyzed according to the linear elastic theory. In linear elastic theory, calculations are made with the assumption that building materials show linear-elastic behavior against tensile and compressive stresses.

For the load-bearing masonry wall of the building, assuming linear elastic behavior under pressure stress is an approach that can give realistic results. Although there is no similar situation for tensile stresses, linear elastic behavior approach is important in determining the areas of the wall subjected to tensile stresses and taking precautions against tensile stresses (against cracks that may occur) in these regions. The loads used on the three-dimensional model in the analysis of the structure are listed below.

- Self (Dead) Loads: In the calculations, the self-weights of the building are taken into account and these loads are automatically included in the calculation by the program.
- Live Loads: In TS 498, a value of q = 5 kN/m^2 is given as live load in residential buildings. This load value is defined as the uniformly distributed load on the floors.
- Earthquake Loads: Both the equivalent earthquake load method and the earthquake spectrum load method were used in the calculation of the earthquake effects of the structure.

Spectral acceleration analysis is used in earthquake analysis of wooden masonry buildings in the Earthquake Code. This was the case when the coefficient R could be taken as 2.5. It has been made using the spectral curve according to the soil class and earthquake zone degree used in spectral analysis. Earthquake loads for both principal directions (X and Y directions) of the building were included in the analyzes separately. The existing load-bearing walls of the building are made of bricks.
The characteristic values given for the walls are given in the table below.

Table 1. Characteristic values given for walls

Physical Size	Value
Specific Weight	18 kN/m^3
Pressure Strength	1.000 kN/m^2
Elasticity Module	2 ile 4.000.000 kN/m^2
Tensile Strength	100 ile 150 kN/m^2

First class pine will be used for the wooden element. The mechanical properties of the material are given below.

Table 2. Mechanical properties of wooden elements

Physical Size	Value
Specific Weight	8 kN/m^3
Pressure Strength	11.000 kN/m^2
Elasticity Module	10.000.000 kN/m^2
Tensile Strength	10.000 kN/m^2

The proposed equations for carbon fiber reinforcement design showed that the design compressive strength f_{mcd} for elements subjected to the lateral confining pressure f_1 can be written as follows:

$$f_{mcd} = f_{md} + k' \cdot f_1' \quad (1)$$

where f_{md} represents the design compressive strength of unconfined masonry, k' is a non-dimensional coefficient and f_1' is the effective lateral confining pressure [2]. The coefficient k' can assume different values depending on the material and the typology of the applied reinforcement. For carbon fiber reinforcement, the value of k' is indicated as $g_m/1250$ where g_m is the specific weight of masonry expressed in kg/m^3. Where k_{eff} is the effectiveness coefficient. This value is the product of two terms: k_H and k_V related to the horizontal and vertical effectiveness [2]. The effective pressure f_1' is expressed in the Standard as:

$$f_1' = k_{eff} \cdot f_1 = k_H k_V f_1 \tag{2}$$

The parameters used are shown below.

- Ground acceleration A = 0.4 g
- Earthquake 1st degree and ground 2nd degree
- Significance factor I = 1.4
- Reduction coefficient = 1

The graphics and other parameters found after these values are entered into the program are shown in Figure 1 and Figure 2.

In the analysis, the regions where tensile and compressive stresses more than the stone wall can carry were determined and spectrum values of the region are given both graphically and numerically. This spectrum has been used to examine the most unfavorable situation for the existing historical building.

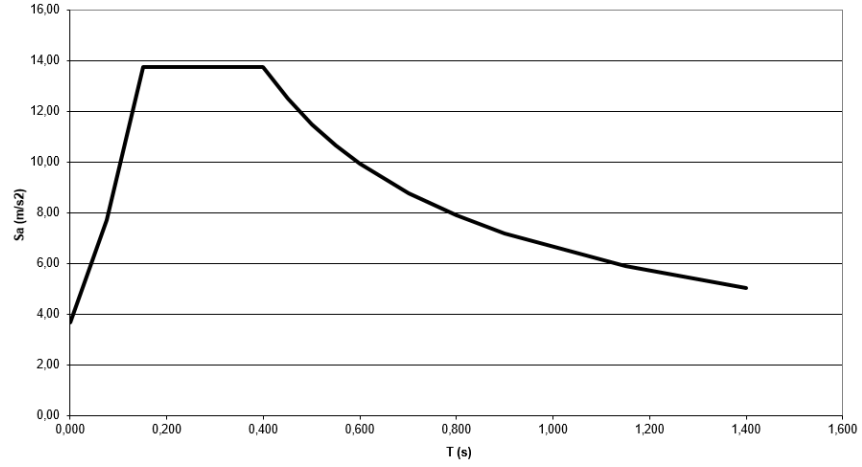

Figure 1. Evaluation response spectrum

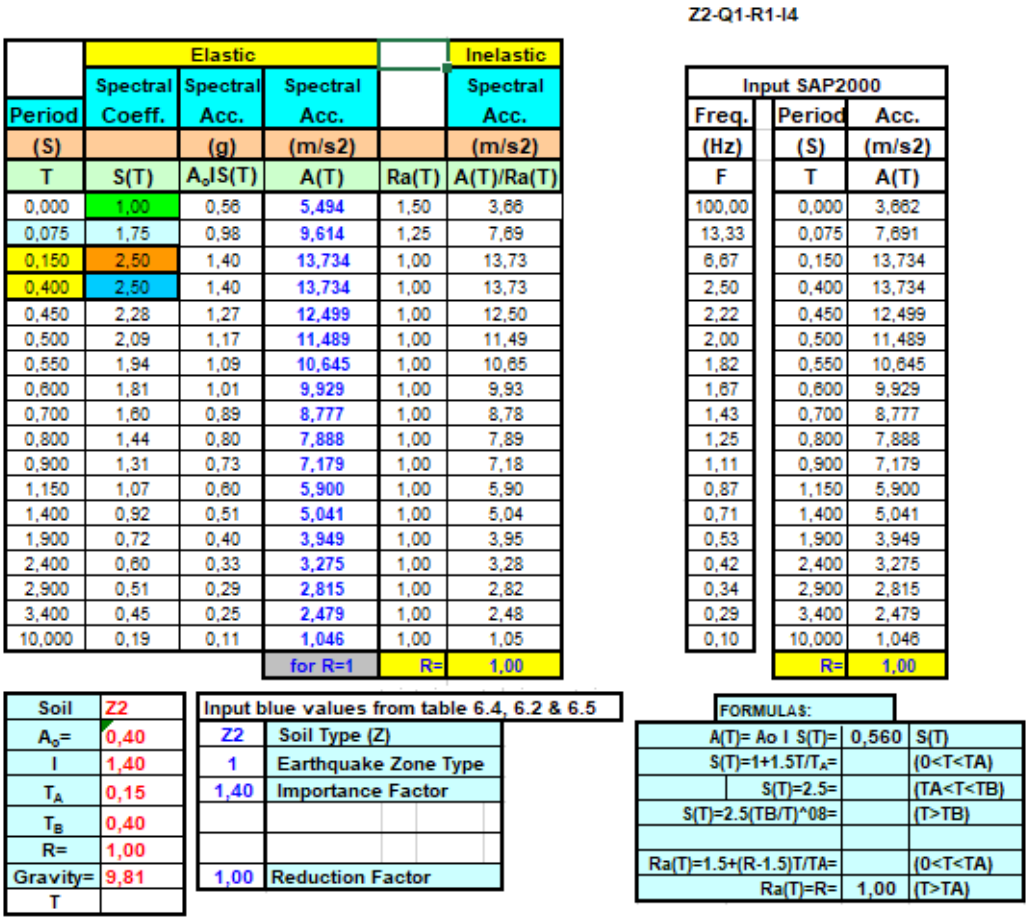

Z2-Q1-R1-I4

Period	Elastic Spectral Coeff.	Elastic Spectral Acc.	Elastic Spectral Acc.		Inelastic Spectral Acc.
(S)		(g)	(m/s2)		(m/s2)
T	S(T)	A_oIS(T)	A(T)	Ra(T)	A(T)/Ra(T)
0,000	1,00	0,56	5,494	1,50	3,66
0,075	1,75	0,98	9,614	1,25	7,69
0,150	2,50	1,40	13,734	1,00	13,73
0,400	2,50	1,40	13,734	1,00	13,73
0,450	2,28	1,27	12,499	1,00	12,50
0,500	2,09	1,17	11,489	1,00	11,49
0,550	1,94	1,09	10,645	1,00	10,65
0,600	1,81	1,01	9,929	1,00	9,93
0,700	1,60	0,89	8,777	1,00	8,78
0,800	1,44	0,80	7,888	1,00	7,89
0,900	1,31	0,73	7,179	1,00	7,18
1,150	1,07	0,60	5,900	1,00	5,90
1,400	0,92	0,51	5,041	1,00	5,04
1,900	0,72	0,40	3,949	1,00	3,95
2,400	0,60	0,33	3,275	1,00	3,28
2,900	0,51	0,29	2,815	1,00	2,82
3,400	0,45	0,25	2,479	1,00	2,48
10,000	0,19	0,11	1,046	1,00	1,05
			for R=1	R=	1,00

Input SAP2000		
Freq.	Period	Acc.
(Hz)	(S)	(m/s2)
F	T	A(T)
100,00	0,000	3,662
13,33	0,075	7,691
6,67	0,150	13,734
2,50	0,400	13,734
2,22	0,450	12,499
2,00	0,500	11,489
1,82	0,550	10,645
1,67	0,600	9,929
1,43	0,700	8,777
1,25	0,800	7,888
1,11	0,900	7,179
0,87	1,150	5,900
0,71	1,400	5,041
0,53	1,900	3,949
0,42	2,400	3,275
0,34	2,900	2,815
0,29	3,400	2,479
0,10	10,000	1,046
	R=	1,00

Soil	Z2
A_o=	0,40
I	1,40
T_A	0,15
T_B	0,40
R=	1,00
Gravity=	9,81
T	

Input blue values from table 6.4, 6.2 & 6.5	
Z2	Soil Type (Z)
1	Earthquake Zone Type
1,40	Importance Factor
1,00	Reduction Factor

FORMULA$:			
A(T)= Ao I S(T)=		0,560	S(T)
S(T)=1+1.5T/T_A=			(0<T<TA)
S(T)=2.5=			(TA<T<TB)
S(T)=2.5(TB/T)^08=			(T>TB)
Ra(T)=1.5+(R-1.5)T/TA=			(0<T<TA)
Ra(T)=R=		1,00	(T>TA)

Figure 2. Earthquake spectrum

2.1. Finite Element Model

After the three-dimensional model prepared by using technical drawings was transferred to the SAP2000 program, the facade views of the model consisting of 3D shell and bar elements were obtained. Color differences on the model represent elements with different characteristics or features. In the past, there were 4 chimneys in the building and these chimneys were generally destroyed in earthquakes and were built again. Since the rigidity of the structure is higher than these chimneys, problems arise in dynamic analysis. Therefore, during the solution, either the chimneys are removed and analyzed in a separate model or the whole system is analyzed together by giving its mass to zero. Analysis done in this way does not pose a problem.

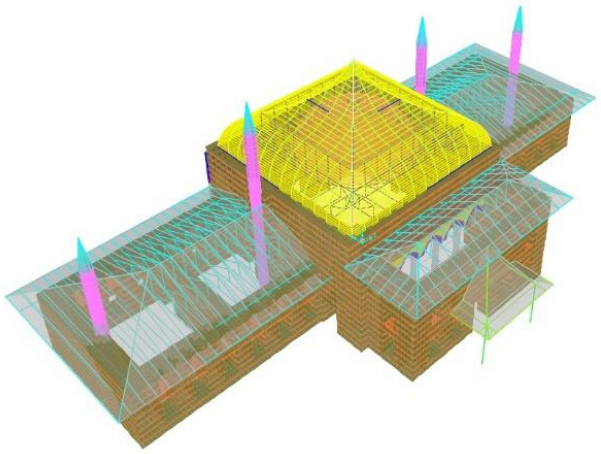

Figure 3. 3D representation of the new structure only, without showing the existing structure

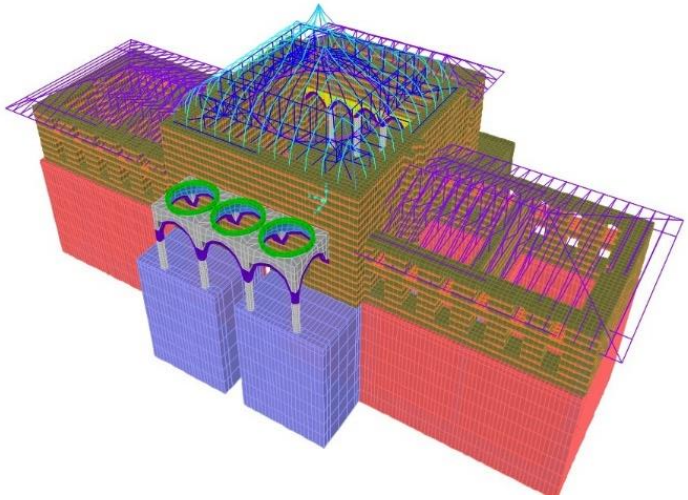

Figure 4. 3D display of the existing building and the new building to be added

In general, the coating and its own weight are given along with the snow load on the roofs. Here the roof weight is 100 kg/m².

2.2. Deformation

Dead, coating, snow, live loads are very little, so it only affects the roof. The general values of the deformations are calculated for the combinations by giving understandable node numbers where desired. Here, the deformation at the top of a roof and the horizontal deformations at the top of the walls are numerically found.

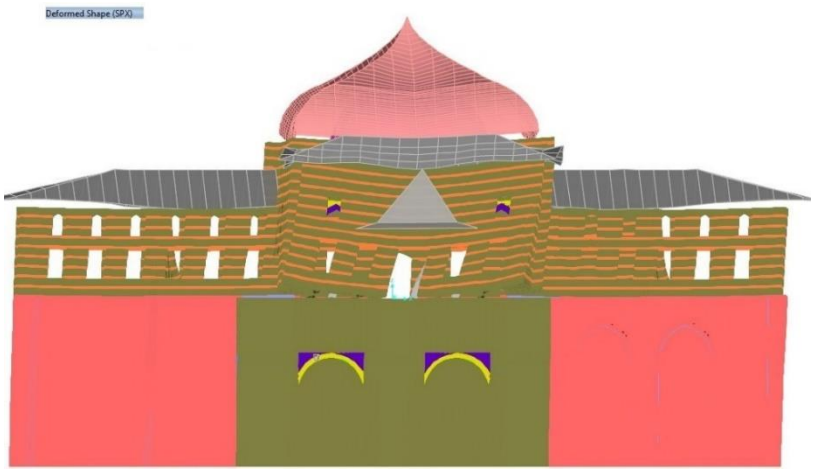

Figure 5. An example form of deformation caused by the structure's own weight and earthquake loads

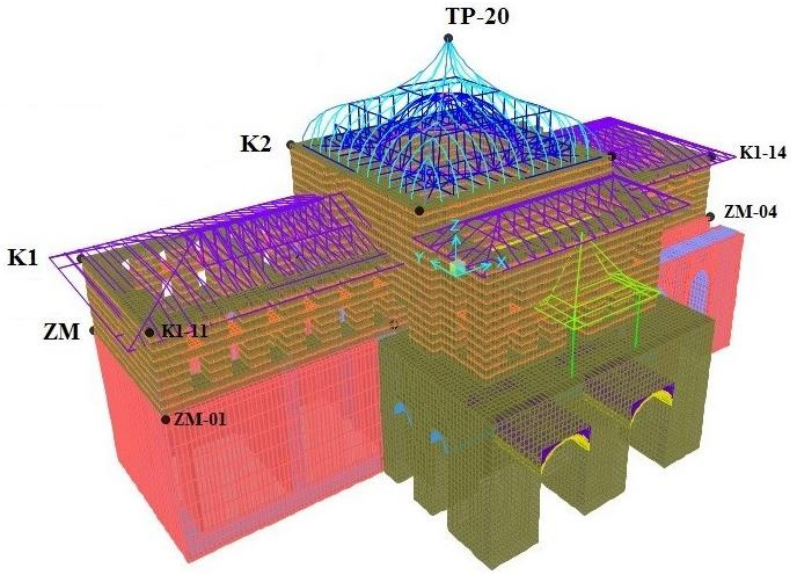

Figure 6: Joint numbers with values shown in the model

2.3. Modal Analysis

Deformations arising from modal analysis were examined. Since the structure is very heavy, the first modes occur on the light roof. But the next modes are given by the building's own mod shapes. In this case, the mass participation factors of the modes do not change, whether in the first or the latter.

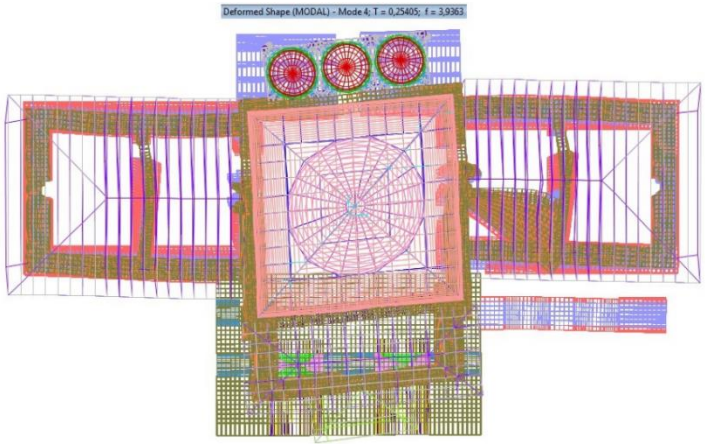

Figure 7. One of the deformed shapes

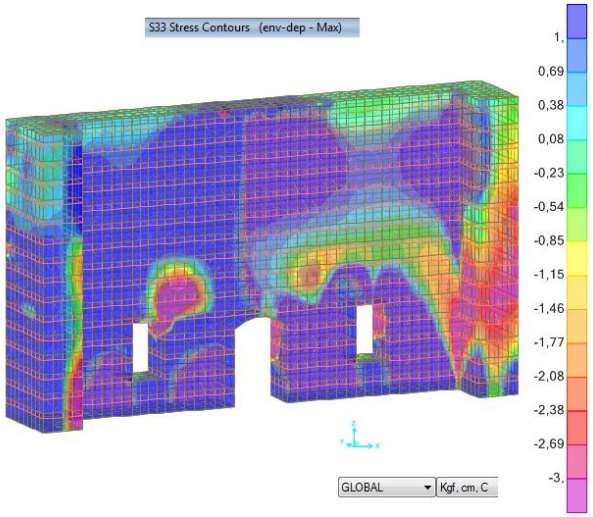

Figure 8. Wall 4 Earthquake loading and S 33 Stress (vertical direction)

In this study, all values of different parameters, which are formed from modal analysis, are calculated. Findings are modal participating mass ratios, modal participation factors, modal periods and frequencies and response spectrum modal information. The walls are modeled as solid (or infill) elements and internal forces are studied in horizontal and vertical directions. In general, vertical stresses are observed in walls under dead and live loads, and the stresses are often far below the capacity of the masonry element. In earthquake situations, these pressures usually increase between 30% and 50%, but the same amount of vertical tension occurs on the other side. If this pull is more than 1-2 kg/cm^2, a slight separation or lift occurs and comes back to its original position depending on the earthquake back and forth movements. If this pull is more than a certain amount in thin and long structures, overturning occurs, which should be

examined in such structures. It is necessary to look at the largest negative values (ie min. Contour) to see the maximum pressure and the largest positive values (max. Contour) to see the maximum pull. As an example, one of them is shown in Figure 8.

3. Conclusion and Suggestions

Building strong and earthquake-resistant walls is to build a wall layer by layer. It is the rule of earthquake-resistant wall construction that every 100-150 cm high layers and smooth stone surfaces in the plane of the layer are formed, the horizontal plane of the wall interlocking one to the other, and a framework with tensile members is formed. In general, horizontal stresses cause cracks in the wall. For this reason, beams in old buildings were placed and if there were no beams, openings would occur on the walls. These walls have cut stone on the outer wall and rubble stone on the inside. The lifespan of these tensile members is about 300 years, but in ancient times these walls were rebuilt using the same techniques. In this structure, the walls are modeled as solid elements and internal forces are viewed in horizontal and vertical directions.

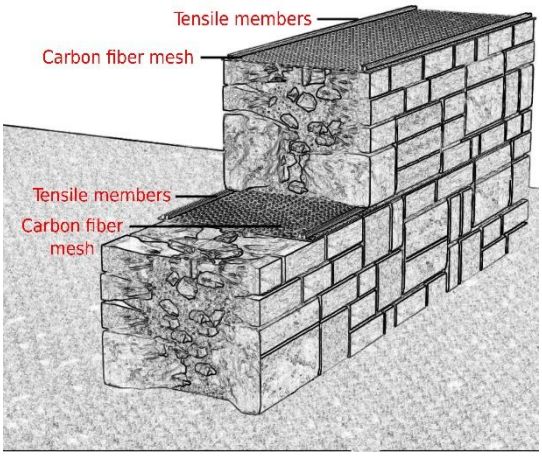

Figure 9: Placement of carbon fiber mesh [3]

In this study, a net is recommended to provide a transverse tensile member between the layers, and this is a system that acts as a stirrup to prevent the wall from opening laterally. Placed wooden beams generally do this task, but opening in case of decay is an inevitable result. Another suggestion is to put a pair of solid beams at the lowest level while constructing the walls. These beams evenly distribute the wall load and prevent cracks if variable settlements occur. In old buildings, wooden beams were generally used as a tensile member. Adhering to the old, these wooden beams were placed in the project. Our recommendation is to place these carbon fiber tensile members together with wooden beams and carbon fiber mesh. These

beams rotted on the walls of the old buildings that we have examined in large quantities and lost their tensile properties. The tapes placed are either a material consisting of carbon fiber or glass fiber [4, 5].

The values obtained in the study of the horizontal tensile amounts of masonry walls are used here in the strengthening calculations. A tensile member equivalent to these tensile amounts was placed. On average, the tensile values on the walls are 1-2 or to 1.5 kg/cm^2. Suppose the wall itself carries the 0.5-1.0 kg/cm^2. For the amount of 1 kg/cm^2 remaining here, 2 pieces of 40 cm wall total tensile amount is 5-6 tons. Here, a total of 4 tensile strength bands of 1 tonne will be placed on both sides of the walls.

The structure is located in the first degree earthquake zone, but since the ground type is good, ie it is built on II and also the importance coefficient of the building is 1.4, there will be a small amount of stress in general. For this, cross cracks are very likely to occur in the walls between windows. On the other hand, these strength bands will be placed in the middle of the wall with 50-60 cm intervals, 2 in each.

Properties of the carbon band;

- There is no corrosion problem seen in steel material in carbon strength bands,
- The carbon strength bands used have an average of 7 times more tensile strength than steel,
- Carbon tapes of 1 to 4 mm thickness and 1 to 4 cm width are easily inserted into the wall joints without disturbing the texture of the structure.
- Strength bands help the wall by carrying not only the tensile stresses, but also the shear stresses occurring in that section.

Carbon tape strengths;

- Tensile strength: 3430 N/mm^2
- Elasticity module: 230000 N/mm^2
- Tape tensile strength: 7480 N

Usage of carbon tape;

- The joints to be opened into the wall are cleaned,
- Double-component polymer is applied to the carbon band in the joint prepared by being fed as much as possible,
- Carbon tapes are stretched and placed in the joint,
- The double component polymer is applied again with a brush on the carbon band, which is placed in the joint and is in physical contact with the joint depth.

- In the polymer application process, care should be taken to polymerize the carbon band and the contact points with the joint without gaps,
- The interior of the joints where carbon tape is laid and polymerized, is filled with a special mortar until the outside of the wall,
- The filled mortar is leveled and smoothed on the wall surface.

The railroad passes next to the building, so the vibrations caused by the rails should be measured with precision instruments and its effect should be examined both in a short time and a long time. Our suggestion is to equip a certain length of these rails with anti-vibration insulators.

References

[1] Ghiga D. A., Tăranu N., Enţuc I. S., Ungureanu D., Scutaru M. C. (2018). Modern Strengthening Techniques for Masonry Structures.

[2] Corradi M., Borri A., Osofero A. I., Castori G. (2015). Strengthening of Historic Masonry Structures with Composite Materials.

[3] Bayraktar A. (2006). Tarihi Yapıların Analitik İncelenmesi ve Sismik Güçlendirme Metodları, İstanbul, Beta Basım.

[4] Carozzi F.G., Bellini A., D'Antino T., de Felice G., Focacci F., Hojdys Ł., Laghi L., Lanoye E., Micelli F., Panizza M., Poggi C. (2017). Experimental Investigation of Tensile and Bond Properties of Carbon-FRCM Composites for Strengthening Masonry Elements.

[5] Babatunde S. A. (2016). Review of Strengthening Techniques for Masonry Using Fiber Reinforced Polymers, Journal of Composites Structures.

Received: 28.10.2019
Accepted: 26.11.2019

Investigation of Istanbul Kartal Example within the Scope of Urban Transformation

Yusuf ÖZ[1], Mehmet Fatih ALTAN[2]

Abstract **-** Due to the increasing migration from rural to urban areas in the world from past to present for various reasons, cities need to be renewed and transformed in future times with the irregular construction occurring in the cities. In this direction, States develop and implement urban transformation policies with various methods.

In the study, the logic of urban transformation is discussed with definitions and the progress of urban transformation in history is mentioned with which aims and methods are carried out. In addition, the data obtained in the incident that occurred with the collapse of a building in Kartal district of Istanbul province in 2019 were mentioned and the construction in the area in question was discussed.

Keywords: *Urban Transformation, Risky Area, The Reserve Building Area, Risky Structures*

Introduction

Cities around the world have seen dramatic and important changes since the second half of the 20th century. Urban transformation in Europe has been supported by varying levels of central government since the late 1960s [1].

[1] *Departmant of Civil Engineering, Istanbul Aydin University, Istanbul, Turkey*
[2] *Departmant of Civil Engineering, Istanbul Aydin University, Istanbul, Turkey, mehmetaltan@aydin.edu.tr, ORCID: 0000-0003-0961-0115*
DOI: 10.17932/IAU.IJEMME.2010.001/ijemme_v10i1004

With the industrialization since the 1980s, many countries have faced urban regression and collapse problems and have implemented urban regeneration strategies with the mentality of restructuring as a way out of this crisis situation [2].

Turkey's urban renewal policies are currently applied in many cities. However, Istanbul, which has the feature of being the city with the largest population, is of great importance. The city, which is located in the earthquake zone, has survived many earthquakes in centuries and has great risk in terms of recurrence in the coming years. Accordingly, Istanbul, the city with the highest migration from the village to the city, is the capital of the country in the unhealthy and illegal construction. One of the most important examples is the migration of a house in the Kartal district. For many reasons, this unhealthy building has lost a large number of people.

1. CONCEPT OF URBAN TRANSFORMATION

Urban transformation; considering the urban problems and urban needs, it is the creation of a viable road map after examining the spatial, social and economic characteristics of a region. It is defined as the reorganization of plans, ownership and functions for the improvement of urban parts that have worn out, deteriorated, risk of earthquake or have become an economic, social and structural collapse area such as slum areas, illegal construction areas, old industrial sites [3].

Risky area in the Law No. 6306 on the Transformation of Areas Under Disaster Risk published in the Official Gazette dated 31.05.2012 and numbered 28309; It refers to the area determined by the President and at risk of causing loss of life and property due to the ground structure or construction on it. Reserve site; It refers to the areas determined by the Ministry or depending on the demand of TOKI or the Administration or to be used as a new settlement area in the applications to be carried out in accordance with the law numbered 6306. Risky structure; It refers to the structure within or outside the risky area, which has completed its economic life, or has been identified on the basis of scientific and technical data that it is at risk of collapse or severe damage [4].

1.1. History Of Urban Transformation

City-related policies in the 1970s; It focuses on issues such as urban poverty, housing need, increased unemployment and long-term unemployment [5]. The adoption of a private sector-weighted urban transformation model in America by the governments in Europe in the 1980s started a new process [6]. With this process, the way for local governments to start making more partnerships with the private sector has been opened. In the 1990s, local people were integrated with the public-private sector, for the first time, multi-sector and multi-actor partnerships emerged. However, the emergence of this partnership has created

a governance system that few people know at the local level and is becoming more and more complex [7]. In the 2000s, while concepts such as Urban Renaissance and Urban Power Association emerged, sustainability, diversity and local people parameters were effective in urban transformation [8].

A major problem with the proclamation of the Republic of Turkey the city, has been the reconstruction of cities ravaged during the war. This situation was also the main subject of the urban transformation actions of the period [9].

Another legal regulation made within the scope of combating illegal housing zones is the Slum Law No. 775, which came into force in 1966 and aims to transform slum areas into regular residential areas.[10] Within the boundaries of this law, 640 slum prevention areas were determined in 20,000 hectares of land and 30,672 houses were built for low-income families. In addition to this, within the scope of the aid to the self-builder, 40,000 houses were provided. Besides, 808 reclamation areas were defined in 16,000 hectares of land, and infrastructure services were provided for these areas, while 202 purging areas in 1,325 hectares of land were cleared of slums [11].

The latest legal development related to urban transformation is the Law on Transformation of Areas under Disaster Risk numbered 6306, dated 16.05.2012 [9]. The purpose of the law; In areas where there are risky structures other than these areas along with disaster risk areas, procedures for improvement, liquidation and renewal are defined to constitute their safe living environment.

1.2. Aims Of Urban Transformation

Urban transformation, by its field of activity and nature, can affect the structure of the existing city and the physical, social and economic future of the people living there, and consequently to all the traditions of the city [12]. Urban transformation should be designed to serve five main purposes.

1. Urban transformation projects should investigate the causes of social disruption and make recommendations to prevent this deterioration.
2. Urban transformation projects should enable the city to be redeveloped according to the new physical, social, economic, environmental and infrastructure needs emerging in the rapidly growing, changing and deteriorating texture of the city.
3. The economic development model should be designed with the feature of enhancing urban welfare and quality of life.
4. Strategies that will bring economic vitality back into urban parts, which in urban areas that have become areas of physical and social collapse, should be developed and thus, it is aimed to increase the urban welfare and quality of life.

5. Strategies should be put forward for the most effective use of urban areas and to avoid unnecessary urban spread.

In Urban Transformation projects, one or more of these goals may come to the fore, depending on the characteristics of the region's problems and potentials [13].

2. ISTANBUL CITY KARTAL DISTRICT URBAN TRANSFORMATION EXAMPLE

The history of Istanbul dates back to 8,500 years ago and has been the capital of three universal empires, such as the Roman, Byzantine and Ottoman Empires. The area of Istanbul, which takes its name from the city and is located on the peninsula between Haliç and Marmara, is 5712 km². According to Turkish Statistical Institute data, the population of Istanbul is 15 million 519 thousand 267 people in 2020.

In Figure 2, the current general structure of Istanbul is shown, yellow areas show urban settlement areas, purple regions show industrial areas and finally, green areas indicate agriculture and green areas. Considering the current structure of Istanbul, the excess of green areas stands out, and the residential areas are predominantly concentrated in the coastal regions of the Bosporus overlooking the Marmara Sea.

Figure 2. Istanbul's Existing Urban Area

Kartal; it is one of the important districts of Istanbul and approximately 3.12% of the total population of Istanbul live here. Its old name is called "Kartalimen" and its history dates back to the 6th century. The total number of buildings is 54.368 and the number of buildings declared as risky buildings within the scope of

Law No. 6306 is 4.109. The district, which has a surface area of 278 km², consists of 20 neighbourhoods. Orhantepe neighbourhood, one of these neighbourhoods, constitutes 6% of the total population of Kartal district.

When Orhantepe District is analysed in general, it is observed that the building is not high-rise and is on the average of 5-6 floors. It was determined that the buildings were built between 1982-1994. Accordingly, when the floor numbers and construction years of the buildings in the neighbourhood are taken into consideration and the ground coefficients are added to the results obtained from the core samples taken from risky structures, the map in figure 6 appears. Areas with intensive risk generally show structures built before the 2007 earthquake regulation, structures built before 2000, when the ready-mixed concrete was widely used, and structures that did not receive engineering services under the building inspection law numbered 4708, which came into force in 2001. When these results are combined with the population, figure 7 occurs. In this analysis, taking into account the settlement of the population, the condition of the distribution of the density by region is examined. When the two results are combined, on average, the data reveal that the same regions pose a risk. In any disaster, these regions will be heavily affected.

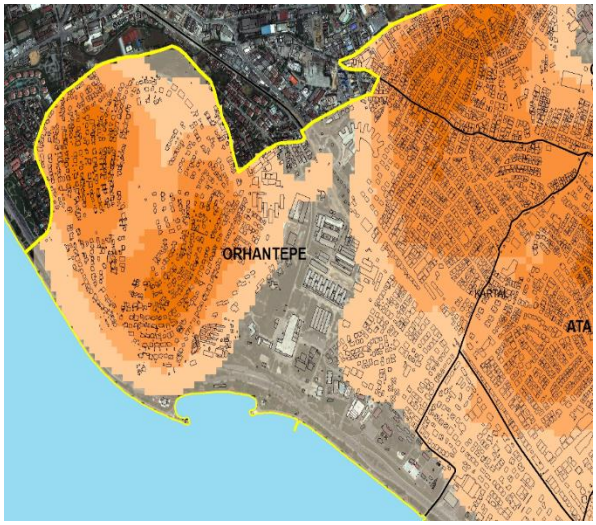

Figure 6. Current Structure Stock Risk Distribution

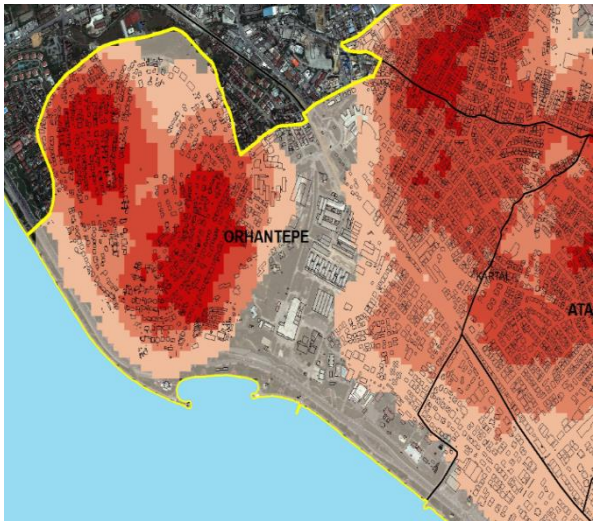

Figure 7. Distribution of Population at Risk

The building on the block number 12580 and 101 parcels located in Orhantepe District collapsed at an unexpected date on 06.02.2019 and 21 people died due to dent and 14 people were taken out from the dent. The mentioned structure was built in 1992 with a total of 9 floors, including basement + ground + 7 normal floors. In the license certificate of the building dated 20.10.1992, there is a 7-storey construction permit,

including 1 basement floor + ground floor + 5 normal floors. The building was built as 2 floors more in violation of the license given by the relevant administration. Basement and ground floors are used for commercial purposes and other normal floors are used for residential purposes. Basement and ground floors are used for commercial purposes and other normal floors are used for residential purposes. The mentioned structure consists of 14 residences and 3 commercial units. The parcel area is 493 m2 and the construction area is 1122 m2 according to the current zoning plan. However, the current construction area of the building is 2209 m2 with illegal floors.

Figure 8. Yeşilyurt Apartments Before Collapse

Figure 9. Yeşilyurt Apartments After Collapse

The building was designed as basement + ground + 5 normal floors in its project in 1992, and the concrete class was designed with B160 and single foundation system according to 1985 TS 500. In the investigations made on the building wreckage, it was observed that unstructured and unwashed sea sand was used in concrete and there was rust in concrete steel.

With the collapse of the mentioned building, firstly observational determinations were made in 10 buildings in 12528 block, 97, 98, 175, 176 parcels, 12580 block 100, 102, 103, 118, 120, 121 parcels in order to be examined within the scope of Law on Transformation of Areas under Disaster Risk by the Ministry of Environment and Urbanization and the implementation regulation.

Table 1. Observational Report of The Reserve Building Area

Apartment Name	Constructional Use	Structural System	Visual Quality	Weak Storey	Heavy Cantilever	Short Column Effect
Ünal	House	Reinforced Concrete Frame	Medium	No	Yes	No
İhya	House	Reinforced Concrete Frame and Concrete Shear Wall	Medium	No	Yes	No
Karalar	Mix	Reinforced Concrete Frame	Medium	No	Yes	No
Potur	House	Reinforced Concrete Frame	Medium	No	Yes	No
Uzunlar	Mix	Reinforced Concrete Frame	Medium	No	Yes	No
Nuri Bey	House	Reinforced Concrete Frame and Concrete Shear Wall	Medium	No	Yes	No
Bahar	Mix	Reinforced Concrete Frame	Medium	No	Yes	No
Anadolu	Mix	Reinforced Concrete Frame	Medium	No	Yes	No
Uğur	House	Reinforced Concrete Frame	Medium	No	Yes	No
Çam	Mix	Reinforced Concrete Frame and Concrete Shear Wall	Medium	No	Yes	No

As a result of observational determinations, it is understood that 5 buildings are residential + commercial and 5 buildings are housing. It is seen that the vast majority of buildings are built as reinforced concrete frames. Although the visual quality of the buildings is medium, the building order is separate. There is heavy cantilever in all buildings. The soft floor and short column effect were not observed.

After observational determinations from the mentioned structures, drilling core samples were taken within the scope of Law No. 6306 and necessary reinforcement stripping was done. As a result of the examination of the data obtained; It has been determined that the buildings are in a position to endanger the safety of life and property, and that there is intense deformation in the buildings, and accordingly, the buildings located in the mentioned parcels except İhya and Çam Apartments have been declared as "Risky Buildings" within the scope of Law No. 6306. The buildings identified as Risky Buildings were immediately evacuated by the authorities to avoid any danger and demolition of the buildings was carried out.

Figure 11. The View After Removal of The Wreckage of Yeşilyurt Apartments

The Reserve Building Area was declared on 11.03.2019 within the scope of Law No. 6306, in order to prepare Yeşilyurt Apartments and the surrounding buildings for earthquake risk, and to provide a liveable area for the protection of life and property security. The 1/1000 scale Implementation Development Plan change and plan disclosure report for the mentioned Reserve Structure Area was approved on 14.03.2019.

Figure 13. The Reserve Building Area

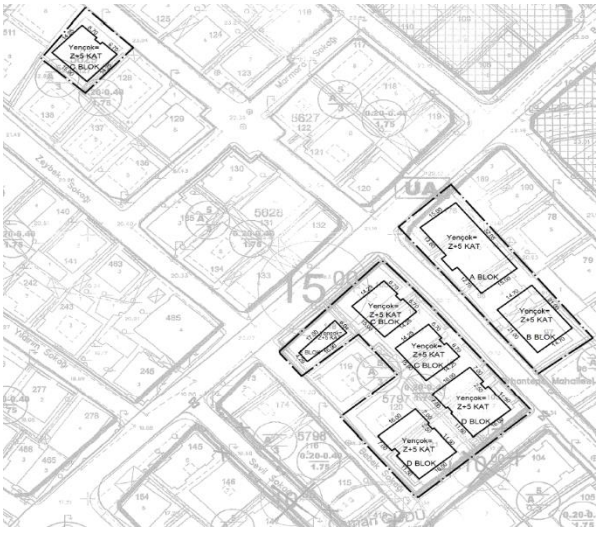

Figure 14. The Reserve Building Area Plan

The buildings within the borders of the Reserve Building Area consist of 129 residences and 29 workplaces. Following the announcement of the Reserve Building Area and the planning processes, the construction process of the construction in the area was started by TOKİ. Along with the mentioned project, 105 houses and 25 workplaces are produced. Approximately 11 months after the date of the incident, 06.02.2019, residences and workplaces were delivered to the beneficiaries on 23.01.2020.

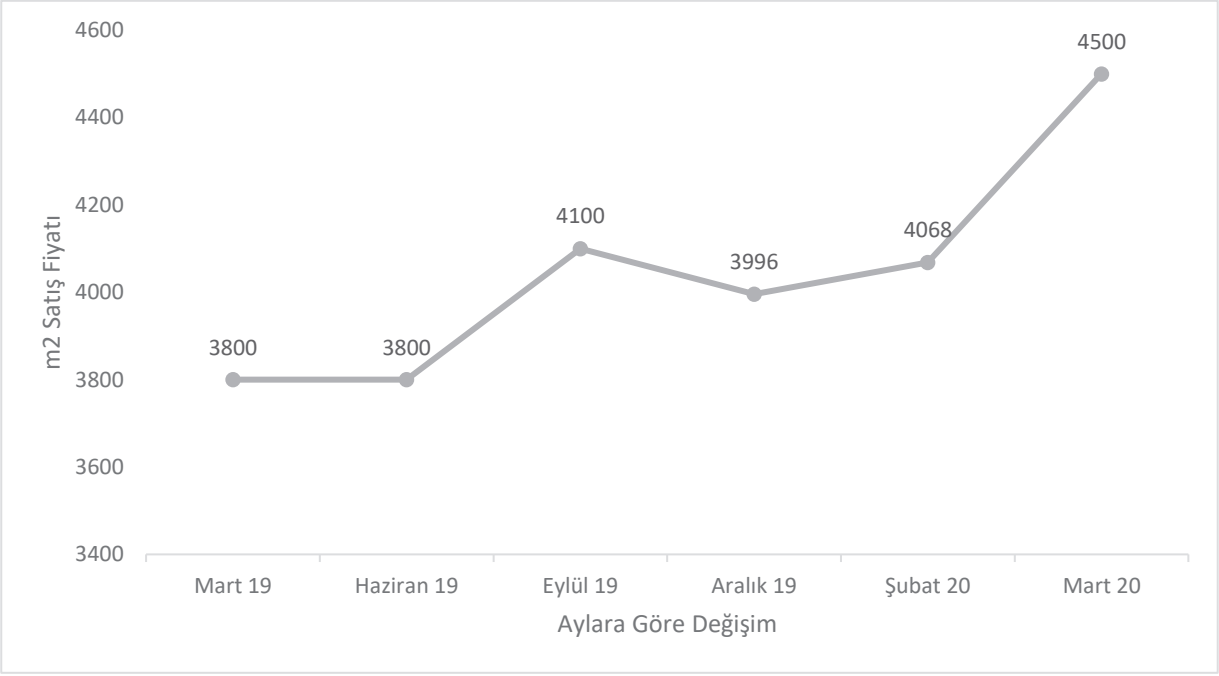

Figure 15. Orhantepe District Real Estate Index

After the delivery of the houses and workplaces, a significant change was observed when the real estate values statement around the area where the crash occurred. After the apartments were handed over to the beneficiaries in February, a significant increase was observed in March.

RESULT

In the 19th century, when the industrial revolution took place in Europe, all policies have changed and especially agricultural policy has entered into a great change and industry has been focused, and as a result, migration from rural to urban areas has increased. With the increase in immigration to the cities, unplanned urbanization started to occur. As a result, an unhealthy city has emerged for people, in this direction, the need for urban transformation in Europe has emerged and urban transformation practices have gained importance.

In our country, the first steps of urban transformation were taken in the 19th century, the last century of the Ottoman State. The first steps were started to be taken in Aksaray in 1854 and it was tried to be extended by various laws with the 1960s. The first legal regulation issued with the expression of Urban Transformation is the Law on Transformation of Areas under Disaster Risk dated 16.05.2012 and numbered 6306. With this law, concepts such as Risk Area, Reserve Structure Area and Risky Structure have directed the transformation.

As a result of the collapse of a building in Kartal district of Istanbul province, 21 people died under the rubble. In this incident, two times more floors have been raised in violation of the license and its annexes given by the relevant administration, and the use of building materials that do not comply with the standards has created an environment for the dentist. Then, with the drilling core samples taken from the surrounding buildings, the buildings were declared as Reserve Building Area and the transformation was started, and new buildings were built within 11 months from the date of demolition and delivered to the beneficiaries

In the studies carried out in the buildings where the collapse occurred and the 10 buildings around it, it was observed that almost all of the structures were used in unstructured and unwashed sea sand. In addition, considering the construction date of the buildings, it was observed that no ready-mixed concrete was used, no engineering services and no S420 ribbed iron was used, and these irons were exposed to great corrosion. It has been observed that similar techniques and materials were used in the buildings since it was built on similar dates in the mentioned settlement unit, and it is obvious that this will bring great destructions during a disaster. Accordingly, this situation has revealed that urban transformation is too important to be ignored.

Conclusion

There are many buildings like this and so on, and urban transformation needs to be accelerated before similar events occur. Otherwise, it is obvious that it will bring unavoidable material and moral results and it is of great importance that states change their main policies within this scope.

REFERENCES

[1] Atkinson, R. ve Moon, G. (1994) Urban Policy in Britain: The City, the State and the Market, London: Macmillan

[2] Urban Task Force (1999) Towards an Urban Renaissance, London: E and FN Spon.

[3] T. Alparslan ve G. Kanal. (2017, 24 Eylül). Kentsel Dönüşüm, [Online]. https://www.makaleler.com/kentsel-donusum-2-3.

[4] Law No. 6306 on the Transformation of Areas Under Disaster Risk published in the Official Gazette dated 31.05.2012 and numbered 28309 (2012).

[5] Özer, Y. E. Yönten, A. ve Yılmaz, F.. (2013). Afet Riski Taşıyan Bölgelerdeki Kentsel Dönüşüm Uygulamalarında Sosyo Beşeri Faktörlerin İncelenmesi Üzerine Bir Çalışma: Uzundere Toki Dayanışma ve Yardımlaşma Derneği Örneği. 8. Kamu Yönetimi Sempozyumu, Hatay, http://kisi.deu.edu.tr/yunusemre.ozer/KENTSEL%20DONUSUM.pdf, (11.05.2015)

[6] Keating, M. (1993) "The politics of economic development: political change and local development policies in the United States, Britain, an France", Urban Affairs Quarterly, 28(3), s. 373-396.

[7] Atkinson, R. (2005), "Kentsel Dönüşüm, Ortaklıklar ve Yerel Katılım: İngiltere Deneyimi", D: Özdemir, P. Özden ve S.Turgut (ed), Uluslararası Kentsel Dönüşüm Uygulamaları Sempozyumu, Küçükçekmece Belediyesi Yayınları s. 87-98.

[8] Lees, L. (2003) "Vision of urban renaissance: the Urban Task Force report and the Urban White Paper", R. Imrie ve M. Raco (ed), Urban Renaissance? New Labour, Community and Urban Policy, The Policy Presss, Bristol

[9] Tekeli, İ., Türkiye'nin Kent Planlama ve Kent Araştırmaları Tarihi Yazıları, Tarih Vakfı Yurt Yayınları, İstanbul, (2010).

[10] Law No. 775 on the Anti-squatting Law published in the Official Gazette dated 20.07.1966 and numbered 12362 (1966).

[11] Görgülü, Z., Hisseli Bölüntü İle Oluşan Alanlarda Yasallaştırmanın Kentsel Mekâna Etkileri, YTÜ Mimarlık Fakültesi Yayınları, İstanbul, (1993).

[12] http://www.arkitera.com/g67-kentsel-donusum.html?year=&aID=792

[13] Roberts, P. (2000), The evolution, definition and purpose of urban regeneration. P. Roberts ve H. Sykes, (Ed.), Urban regeneration a handbook .London: SAGE Publications.

INTERNATIONAL JOURNAL OF ELECTRONICS, MECHANICAL AND MECHATRONICS ENGINEERING

Submission Instructions

The scope of International Journal of Electronics, Mechanical and Mechatronics Engineering (IJEMME) covers the novel scientific papers about Electronics, Image Processing, Information Theory, Electrical Systems, Power Electronics, Control Theory, Embedded Systems, Robotics, Motion Control, Stochastic Modeling, System Design, Multidisciplinary Engineering, Computer Engineering, Optical Engineering, Design Optimization, Material Science, Metamaterials, Heat and Mass Transfer, Kinematics, Dynamics, Thermo-Dynamics, Energy and Applications, Renewable Energy, Environmental Impacts, Structural Analysis, Fluid Dynamics and related topics of the above subjects.

IJEMME is an international journal published twice a year (January and July). Manuscripts reporting on original theoretical and/or experimental work and tutorial expositions of permanent reference value are welcome. IJEMME Editorial Board is authorized to accept/reject the manuscripts based on the evaluation of international experts. The papers should be written in English.

The manuscript should be sent in electronic submission via IJEMME paper submission system of web address (www.aydin.edu.tr/ijemme)

Submission instructions of manuscripts.

Page Design: Text body area is (17mm x 24mm). 30 mm margin from top, 20 mm from down and 25 mm margin should be left on right/left sides.

Title should be in 16 pt. bold, capital letters with Times New Roman font in Microsoft Word format. Authors' names, affiliations, e-mail addresses should follow the title after double line spacing with authors' names and surnames in lower case except first letters in 14 pt, the rest is 10 pt. italic.

Abstract should not exceed 200 words with the word "Abstract" in 10 pt. italic, bold, abstract text in 9 pt. italic, all in Times New Roman font in Microsoft Word format.

Key Words not exceeding 5 should be in bold.

Document Character: Subtitles should be in 10 pt. bold, capital letters and text body 10 pt. both with Times New Roman font in Microsoft Word format. The manuscripts should be written on a single column, be double spaced with single line spacing between paragraphs. The subtitle of the first section should start after a single space following the keywords, the other subtitles also with a single line space following the text, there should also be single line spacing between the previous text and the subtitle.

Conclusion: section should have a title written in 1o pt. bold, capital letters and the text in 10 pt. all in Times New Roman font in Microsoft Word format.

Reference numbers should be given in brackets as illustrated below:

Referencing books:
[1] Özsu M., T, Valduriez, P., *Principles of Distributed Database Systems*, Prentice Hall, New Jersey, 128-136,1991.

Referencing papers:
[2] G. Altay, O. N., Ucan, "Heuristic Construction of High-Rate Linear Block Codes," *International Journal of Electronics and Communications (AEU),* vol. 60, pp.663-666, 2006.

Page number is to be placed at the top left corner of each page with pencil.
Length of the Manuscript should not exceed 20 pages excluding Figures and Tables.

INSTRUCTIONS ABOUT THE ACCEPTED MANUSCRIPTS:

Page Design: Text body area is (195mm x 275mm). 30 mm margin from top, 20 mm from down and 25 mm margins should be left on right/left sides.

Title should be in 16 pt. bold, capital letters with Times New Roman font in Microsoft Word format. Authors' names, affiliations, e-mail addresses should follow the title after double line spacing with authors' names in lower case and surnames in capital letter in 14 pt. the rest in 10 pt. in the same format.

Abstract should not exceed 200 words with the word "Abstract" in 12 pt. italic, bold, abstract text in 9 pt. italic, all in Times New Roman font in Microsoft Word format.

Key Words not exceeding 5 should be in 9 pt. bold.

Document Character: Subtitles should be in 10 pt. bold, capital letters and text body 10 pt. both with Times New Roman font in Microsoft Word format. The manuscripts should be written on two columns, be single spaced with single line spacing between paragraphs. The subtitle of the first section should start after a single space following the keywords, the other subtitles also with a single line space following the text, there should also be single line spacing between the previous text and the subtitle.

Sections: Formulas should be numbered sequentially. Referring to formulas should be as Eqn (.). Figures and Tables should be placed into the text body and captions for both should be 10 pt. Table numbers and captions should be placed before the Table. If necessary, both columns may be used for large Figures and Tables.

Conclusion section should have a title written in 12 pt. bold, capital letters and the text in 10 pt. all in Times New Roman font in Microsoft Word format. Conclusion should not be a version of the Abstract.

Reference numbers should be given in brackets as illustrated below:

Referencing books:
[1] Özsu M., T, Valduriez, P., *Principles of Distributed Database Systems*, Prentice Hall, New Jersey, 128-136,1991.

Referencing papers:

[2] G. Altay, O. N., Ucan, "Heuristic Construction of High-Rate Linear Block Codes*," International Journal of Electronics and Communications (AEU),* vol. 60, pp.663-666, 2006.

Short Biography of the authors should follow references after a single line space, names in 9 pt. surnames in 9 pt. and the text in 9 pt. The text should not exceed 100 words.

CORRESPONDENCE ADDRESS:

Editor in Chief
Prof. Dr. Hasan Alpay HEPERKAN
Istanbul Aydın University, Faculty of Engineering
Mechanical Engineering Department
Florya Yerleskesi, Inonu Caddesi, No.38, Kucukcekmece, Istanbul, Turkey
Fax: +90 212 425 57 59 - Tel: +90 212 425 61 51 / 22001
E-mail: hasanheperkan@aydin.edu.tr

Prepared by
Instructer:Saeid KARAMZADEH
Engineering Faculty
Electrical and Electronics Eng. Dept.
Inonu Caddesi, No.38, Florya, Istanbul, TURKEY
E-mail: saeidkaramzadeh@aydin.edu.tr

Published by
Istanbul Aydın University
Graphic Design Department